SEGMENTATION OF MEDICAL IMAGES USING LEVEL SET METHOD

A DISSERTATION

Submitted in partial fulfillment of the requirements for the award of the degree of

MASTER OF TECHNOLOGY

in

ELECTRICAL ENGINEERING

(With Specialization in Measurement and Instrumentation)

By

NAGARATNAMMA.K

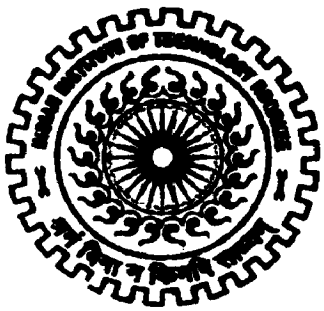

DEPARTMENT OF ELECTRICAL ENGINEERING
INDIAN INSTITUTE OF TECHNOLOGY ROORKEE
ROORKEE - 247 667 (INDIA)
JUNE, 2007

I.D. No.-M.T. 395/2007-28/RSA

INDIAN INSTITUTE OF TECHNOLOGY ROORKEE
ROORKEE

CANDIDATE'S DECLARATION

I hereby declare that the work, which is being presented in this dissertation entitled **"SEGMENTATION OF MEDICAL IMAGES USING LEVEL SET METHOD"** in the partial fulfillment of the requirements for the award of the degree of **Master of Technology in Electrical Engineering** with specialization in **Measurement and Instrumentation**, submitted in the **Department of Electrical Engineering, Indian Institute of Technology Roorkee**, Roorkee is an authentic record of my own work carried out during a period from July 2006 to June 2007 under the supervision of **Dr. R.S.Anand**, Associate Professor, Electrical Engineering Department, Indian Institute of Technology Roorkee, Roorkee.

The matter presented in this thesis has not been submitted by me for the award of any other degree of this or any other Institute.

Date: 29/6/07
Place: Roorkee

K. Nagaratnamma
(NAGARATNAMMA.K)

CERTIFICATE

This is to certify that the above statement made by the candidate is correct to the best of my knowledge and belief.

29.06.07
Dr. R.S.Anand
Associate Professor,
Department of Electrical engineering,
Indian Institute of Technology Roorkee,
Roorkee-247667.

Date 29/6/07
Place: Roorkee

ACKNOWLEDGEMENTS

I express my foremost and deepest gratitude to **Dr. R.S.Anand**, Associate Professor, Department of Electrical Engineering, Indian Institute of Technology Roorkee, Roorkee for his valuable guidance, support and motivation throughout this work. I have deep sense of admiration for his innate goodness and inexhaustible enthusiasm. The valuable hours of discussion and suggestions that I had with him have undoubtedly helped in supplementing my thoughts in the right direction for attaining the desired objective. I consider myself extremely fortunate for having got the opportunity to learn and work under his able supervision over the entire period of my association with him.

My sincere thanks to all faculty members of Measurement & Instrumentation for their constant encouragement, caring words, constructive criticism and suggestions towards the successful completion of this work.

I do acknowledge with immense gratitude the timely help and support, which I received from my classmates and the Research Scholars in the "Biomedical Instrumentation Laboratory". I am also thankful to the staff of this Lab for their kind cooperation.

Last but not least, I'm highly indebted to my parents and family members, whose sincere prayers, best wishes, moral support and encouragement have a constant source of assurance, guidance, strength, and inspiration to me.

K. Nagaratnamma

(Nagaratnamma .K)

ABSTRACT

This thesis proposes a novel theoretical framework, namely the curve evolution implementation of the Mumford–Shah objective function for dealing with the image segmentation. This frame work is based on the mathematical properties of the operator. The active contour model without edges based on the Mumford-Shah function is fully dependent on the initial position of the curve; it crosses the required boundaries if the number of iterations are more, and also results in unnecessarily splitting of the curve

In another method, the initial curve which is necessary for the level set method is created by the randomized Hough transform (RHT) which overcomes the limitations of the Hough transform and some morphological operators are also used in pre-processing stage along with the randomized Hough transform. The initial curve which is created by this transform is the basis for total level set method and it effectively overcomes the limitations of the basic method.

The RHT based method does not require reinitialization of the distance function in every step and so speed of this method is increased. With creation of the ellipse in proper position by randomized Hough transform, the required fetal head is detected within few iterations. The performance of this method is measured with the error metric called Hausdorff distance. The speed function of this model is based on the image region and boundary gradient information. The method proposed here combines the randomized Hough transform and active contours without reinitialization to overcome the limitations faced by traditional methods.

CONTENTS

LIST OF FIGURES

LIST OF TABLES

CHAPTER 1
INTRODUCTION

In this chapter, a general view of fetal head detection is presented. Moreover a brief introduction towards ultrasound imaging is given followed by a brief description of the role of image segmentation. Also overview of the approach proposed in this thesis is shortly introduced.

1.1 Ultrasound Imaging

Medical ultrasound, also called sonography, is a mode of medical imaging that has a wide array of clinical applications. The basis of its operation is the transmission of high frequency sound into the body followed by the reception, processing, and parametric display of echoes returning from structures and tissues within the body. One reason for using ultrasound waves, other than the fact that they are inaudible, is that for shorter wavelengths there is less diffraction, so the beam spreads less and smaller objects can be detected. For an obstacle intercepts and reflects a portion of a wave significantly only if the wavelength is less than the size of the object. Indeed, the smallest-sized objects that can be detected are of the order of the wavelength used. With the higher frequencies of ultrasound, the wavelength is smaller, so smaller objects can be detected [1]. The diagnostic use of ultrasound in medicine is also based on the pulse-echo technique, much like sonar. Normally Ultrasound imaging is used in manufacturing and it is having more applications in medicine, especially in obstetrics, where unborn babies are imaged to determine the health of their development.

Ultrasound images are generated using the following basic procedure [2]:

1. The ultrasound system (a computer, ultrasound probe consisting of a source and receiver, and a display) transmits high-frequency (1 to 5 MHz) sound pulses into the body.
2. The sound waves travel into the body and hit a boundary between tissues (e.g., between fluid ,soft tissue and bone).Some of the sound waves are reflected back to the probe, while some travel on further until they reach another boundary and get reflected.

3. The reflected waves are picked up by the probe and relayed to the computer.
4. The machine calculates the distance from the probe to the tissue or organ boundaries using the speed of sound in tissue (1540 m/s) and the time of the each echo's return.
5. The system displays the distances and intensities of the echoes on the screen, forming a two-dimensional image.

In a typical ultrasound image, millions of pulses and echoes are sent and received each second. The probe can be moved along the surface of the body and angled to obtain various views. A high-frequency sound pulse is directed into the body, and its reflections from boundaries or interfaces between organs and other structures and lesions in the body are then detected. By using this technique, tumours and other abnormal growths, or pockets of fluid, can be distinguished, the action of heart valves and the development of a foetus can be examined, and information about various organs of the body, such as the brain, heart, liver and kidneys, can be obtained. Some kinds of tissue or fluid are not detected in X-ray photographs, but ultrasound waves are reflected from their boundaries.

Ultrasonic imaging uses frequencies in the range from 1 to 20 MHz at powers from 0.01 - $200 mW/cm^2$. The ultrasound is generated and received by piezoelectric transducers. The speed of sound waves in the tissues of the human body averages about 1540 m/s (close to that for water). So, the wavelength of a 1 MHz wave is about $\lambda = v/f$ =1540/1x10e6 = 1.5 mm. This wavelength sets the limit to the smallest-sized objects that can be detected. Higher frequencies mean shorter wavelengths, and thus in principle a visualization of finer detail. However, the higher the frequency is, the more the wave is absorbed by the body, and reflections from deeper inside the bodies are lost.

1.2 What is Image Segmentation?

Segmentation sub divides an image into its constituent regions or objects. The level to which the subdivision is carried depends on the problem being solved. That is, segmentation should stop when the objects of interest in an application have been isolated. Thus the Segmentation is a process of extraction of information from an image

in such a way that the output image contains much less information than the original one, but the little information that it contains is much more relevant to the purpose of the task Medical Image Segmentation is the extraction of anatomical structures which are used for diagnosis purpose.

1.3 Why Segmentation?

Doctors and radiologists spend several hours daily analyzing patient images (ie.medical images like CT, MRI ,US images) to Search for patterns in images that are standard and well-known to doctors. The solution for this is doctors and radiologists can teach the computer to recognize abnormalities in medical images. Image segmentation plays a crucial role in many medical imaging applications by automating or facilitating the delineation of anatomical structures and other regions of interest. Quantification by manual tracing of outlines of structures to be studied is tedious, time-consuming and also hampered by significant inter- and intra-observer variabilities. Imaging modalities, which produce multidimensional data sets such as CT and MRI, require the interpretation of tens to hundreds of slices. As a result, there is a great need for segmentation techniques that are robust and are characterized by a high degree of accuracy and precision.

So the Image segmentation is a very challenging and demanding problem in image analysis. Because of the important role it plays in the modern image analysis, many authors have addressed this problem, but universal solution has not yet been found. Medical image analysis is an important part of image analysis applications. With development of complex medical imaging modalities which are capable of producing a large quantity of high-resolution image data, both two dimensional (2-D) and three-dimensional (3 -D), quantitative analysis of such data becomes almost impossible. Physicians would have to spend hours analyzing this data manually without assistance of computer-based methods. Because the patient life or health can be at stake, these programs must be fast and more important very accurate [2].

1.4 Overview of Fetal Head Detection

Measurement of the fetal head circumference and diameters in addition to the femur length is crucial for the estimation of fetal age and growth pattern. Due to the noisy nature of ultrasound images and variation in image acquisition and measurement techniques, manual measurements of these parameters are subject to inter and intra-observer variability. Images of the fetal head exhibit several problems; for example, the presence of other highly echogenic structures adjacent to the head contour and non uniform bone texture, potential measurement errors stem from the deficiency of echoes from head segments parallel to the ultrasound wave propagation direction. This is due to the relatively high reflection coefficient of bone, causing very low transmission of beam power into the bone, and hence, very weak or no signals from lower bone layers. In addition, the acoustic beam deflection at the bone interface causes a change in the wave propagation direction, with the result that very weak echoes are detected by the transducer at the assumed angle of reflection. Accordingly, the head boundaries are difficult to define and trace in a direction perpendicular to the ultrasound beam, likewise measurement of its diameters [1]. The automation algorithms are mainly based on morphological operations for the noise elimination and segmentation phases; to selectively enhance the head contour and diminish other unrelated structures. Automatic head measurements are then performed with optimal accuracy and consistency of the results.

1.5 Literature Review

In 1994 G. K. Matsopoulos and S. Marshal introduced an automatic method which uses a class of nonlinear image processing filters known as morphological operators to connect and isolate the fetal head within an ultrasound image and generate a measurement of its diameter. This measurement is a valuable indicator in estimating the gestational age of the infant. For applying this scheme in an automatic or semi-automatic way as only a priori information about the general size of image features is required [3].

Vicent Caselles proposed a geometric active contour model of active contours for 2D, 3D boundary detection and motion tracking. The technique is based on

active contours evolving in time according to intrinsic geometric measures of the image. The evolving contours naturally split and merge , allowing the simultaneous detection of several objects and both interior and exterior boundaries. The proposed approach is based on the relation between active contours and the computation of minimal distance curves or minimal surfaces in a Riemannian space whose metric is derived from the image [4].

Analysis of ultrasound (US) fetal head images is a daily routine for obstetricians, radiologists and sonographers.The circumference of the outer skull of the fetal head is manually measured by tracing the skull or fitting an ellipse to it with a mouse-like device which is proposed by Athey and Hadlock in 1985.In this method the variations are a major contributor to inaccurate measurements [5]. In addition to the problem of measurement errors and inconsistencies, manual measurements take time and labor which are pointed by Zador et al. 1991;Chalana et al.1996.

To overcome the disadvantages of manual measurements, image-processing and object-recognition techniques have been used for automatic or semiautomatic fetal measurements which are proposed by Salari et al. 1990; Thomas et al. in 1991; Zador et al. 1991; Matsopoulos and Marshall 1994; In 1997 Pathak et al. proposed a method which detects the noncontiguous skull by iterative dilations and the head area was filled by a grow-filling algorithm.

1.6 Objective of the thesis

The main objective of this work has been to apply level set segmentation method to recognize the fetal head contour in the ultrasound image, refine its shape and compensate for different irregularities and to compare the proposed method with the traditional method.

1.7 Organization of the thesis

In this thesis, a quite important problem of fetal head detection is considered and this framework is used to provide solutions to the most requested low level segmentation tasks (image/texture segmentation).

Initially in Chapter 2, a general variational framework is proposed namely the active contour model, which integrates the image dependent characteristics with the shape information sources under a curve based minimization approach. This framework has a very large applicability and can be used to deal with important applications in medical image segmentation. The curve propagation is implemented using the level set theory, which enables numerous nice properties but mainly it can handle automatically the changes of topology.

In chapter 3, the basic Hough transform and its applications are discussed and it also discusses how much effectively the randomized Hough transform overcomes the limitations of the Hough transform. The optimization procedure leads to the propagation of multiple curves (one for each image region) which is implemented using the level set theory.

Chapter 4 presents discussion about randomized Hough transform and active contours without reinitialization and compares this method with traditional method.

In chapter 5 results are presented and relevant discussions are also made on the resulting output.

Finally, in chapter 6 conclusions are presented. The future directions of the work are also suggested.

CHAPTER 2

OVERVIEW OF ACTIVE CONTOURS

This chapter presents a novel variational framework, namely the Active Contours for dealing with image segmentation problems by the propagation of curves. This chapter discusses the need of segmentation in medical images, and the disadvantages of basic methods.The level set method which belongs to one of the active contour classes is introduced in this chapter where the segmentation depends on a curve-based energy framework, which aims at finding a minimal length curve that preserves two main properties:

- It is regular and smooth,
- It is attracted by the boundary points (important boundary-based information),

The propagation of a curve is implemented using the level set theory which consists of a variational framework that deals automatically with changes of topology (splitting and merging), thereby allowing multiple curves to be the result of the evolution of a single initial curve.

2.1 Introduction

For a scientist, an image is an information carrier, but the information of interest may not be always perceivable with the human eye only because of corruption by the noise or simply tied up with the details and information of no interest. In such cases we may have to develop techniques to extract that information which is interested for our applications from the image. This area of image processing is called image analysis. The first and the most important step in image analysis is to segment the image (often referred to as boundary estimation, boundary detection or object localization).Segmentation subdivides an image into its constituent parts. Segmentation algorithms for monochrome images generally are based on one of two basic properties of grey-level values: discontinuity and similarity. The first method partitions an image based on abrupt changes in grey-level (isolated points, lines and edges) while the second method is based on thresholding, region growing and region splitting and merging.

2.2 Types of Segmentation Techniques

In image analysis, segmentation is one of the important and most difficult tasks. This segmentation stage determines the performance of the whole system. There are many ways to classify segmentation techniques for both general applications and specific applications like for MRI, CT, Ultra sound image segmentations. By considering the generality of segmentation, segmentation techniques can be classified into four broad categories namely edge-oriented, region-oriented, active contour model-based, and hybrid approach Figure.2.1 illustrates the taxonomy of segmentation techniques [2, 3].

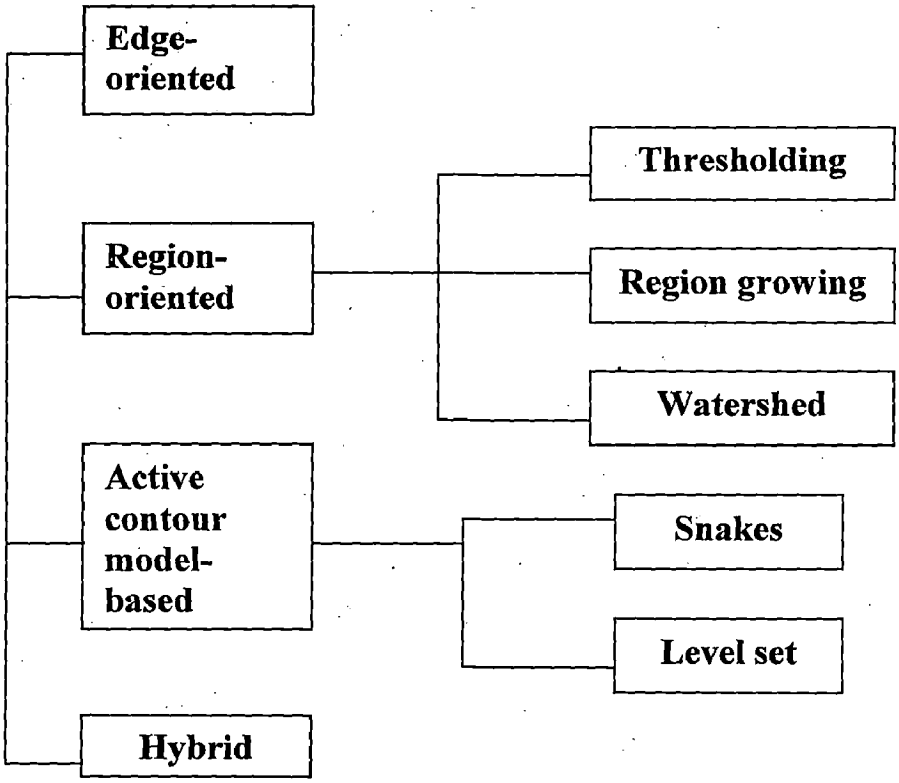

Fig 2.1 Taxonomy of vasculature segmentation techniques

2.2.1 Edge-oriented Segmentation Techniques

In this approach, the edges between regions with different characteristics are derived first; then regions enclosed by the edges are segmented. An edge is the boundary between two regions with relatively distinct intensity properties. Basic approach of most edge detection algorithms is to use a local derivative operator. There are various versions of derivative operators with different approaches and applications, such as Sobel, Laplacian, Canny, Roberts, Prewitt, etc. Because of the nature of the

derivatives, all edge operators are very sensitive to noise. A good solution to this problem is to smooth the image before doing edge detection.

2.2.2 Region-oriented Segmentation Techniques

In this approach, images are segmented into regions of pixels which are having certain similarity (i.e., regions are found directly). There are three principle approaches in this category, namely, thresholding, region growing, and watershed Image.

Thresholding is a process that transforms the grey scale values of an image into binary values. The success of segmenting regions with thresholding depends critically on the selection of an appropriate threshold value. There are three basic ways of selecting the threshold. One is to manually select by a human which can give ideal results in some cases. Another approach is ad hoc in which the threshold value is selecting according to certain rules. For example, the threshold is set to the mean value of the image by utilizing the properties of image histogram. This approach is based on the assumption that different objects in an image have distinct peaks in the histogram. The difficulty of the histogram-based approach is that the assumption is mostly wrong. The intensity distributions of different objects are overlapped.

Region growing starts with a set of pixels called seeds which belongs to the structure of interest and can be selected manually or by an automatic process. One or a few seeds correspond to a region. There may be multiple regions depending on applications. In the region growing process, all the pixels neighboring a seed are examined to see if they are sufficiently similar to the seed according to a homogeneity criterion. If the pixels are similar to a seed, they are added to the region containing the seed and this procedure continues until all the pixels are checked. A limitation of region growing is that it is unstable because it is sensitive to the facts such as the definition of the neighborhood and the choice of homogeneity criterion.

Watershed image is the landscape of image where bright pixels represent mountains and dark pixels represents valleys. In this method the landscape is punctured in some valleys and water is flooded in to fill the valleys and dams are built at points where water coming from different valleys would meet to stop the mixing of the water.

2.2.4 Hybrid Segmentation Techniques

In this approach, the strengths of several segmentation techniques are combined to achieve segmentation. Basically this approach integrates the three categories discussed before by amplifying their strength and reducing their weakness. The trend is that more comprehensive and powerful hybrid segmentation methods are developed [4].

According to the initialization the segmentation techniques can be classified as

1) Semi-Automatic segmentation
2) Automatic segmentation

Some times, the segmentation can be easily misled by undesired edges due to noise and so it makes the fully automatic contour extraction very difficult. And under certain situations, the reliability and accuracy of the extraction algorithm is very important while its automation is not so crucial so then semi-automatic method can be used. In this the initialization is given manually and then computer algorithms are used on that to get reliable segmentation. Thus Semi-automatic contour extraction with minimal user inputs is suitable when reliability and accuracy are more important than automation. But in some applications, the situation is reversed. For example, when many ultrasound images need to be screened, a fully automatic method is more efficient than a semi-automatic one.

2.3 Why Active Contours?

The problem with these basic methods is that the edges found are not necessarily corresponding to boundaries of objects. With the exception of high-quality images from controlled environments, these methods produce spurious edges and gaps. The limitation of these methods is due to their complete reliance on information contained in the local neighborhood of pixels in the image and they ignore both model-based information and higher order organization of the image. Another problem associated with these methods is edge grouping. After extracting edges from the image, they have to be grouped in order to determine boundaries which is usually done by first associating edge elements into edge segments and then by associating segments into boundaries. These methods are considered as low-level methods. Alternatively, in high-

level segmentation methods the priori knowledge about the shape, texture, color, or position of the object in question is included.

2.4 Active Contour Models

Active contour models are an attractive approach to boundary detection in medical images such as: snakes, deformable templates and dynamic contours. Active contours are the curves that deform within digital images to recover object shapes. They are classified as either parametric active contours or geometric active contours according to their representation and implementation. In particular, parametric active contours are represented explicitly as parameterized curves in a Lagrangian formulation. Geometric active contours are represented implicitly as level sets of two-dimensional distance functions which evolve according to an Eulerian formulation. Geometric active contours have many advantages over parametric active contours, such as computational simplicity and the ability to change curve topology during deformation.

2.4.1 What is a Snake?

Snake is a parametric curve defined within the domain of an image whose properties and behavior is specified through a function called energy function. A partial differential equation controlling the snake causes it to evolve so as to reduce its energy. This model corresponds to an elastic curve that is propagated by image forces towards the minimum of an energy generated by an image. Besides, this model introduces some internal regularization constraints, which ensure the regularity of the curve and limit the bending affect. The first snake model was proposed by Kass in 1987. The energy functional which the snake was to minimize in order to achieve equilibrium was defined as following

$$E_{snake} = \int_0^1 \{E_{\text{int}}(v(s)) + E_{image}(v(s))\} ds \tag{2.1}$$

where the position of the snake on the image is represented parametrically by a planar curve $v(s) = (x(s), y(s))$, E_{int} represents the internal energy of the curve due to the bending and the E_{image} represents the image forces pushing the snake toward the desired object.

E_{int} and E_{image} are internal and external forces, respectively and the contour comes to rest when the net effect of the damping, internal, and external forces reaches to zero. The external force is designed to pull an active contour towards the object boundaries. Many types of external forces have been developed in the past, including the well-known pressure force and the Gaussian potential force. The internal force is the sum of elastic and rigid forces defined as follows.

$$E_{elastic} = [\alpha(s,t)X_s(s,t)]_s \qquad (2.2)$$
$$E_{rigid} = -[\beta(s,t)X_{ss}(s,t)]_{ss}$$

Where X_S is the first derivative and X_{SS} is the second derivative of X with respect to s.

The second derivative gives us the rate of convexity or the curvature and the coefficient $\beta(s)$ regulates the rate of change of curve in the direction of normal to its boundary. This term makes the snake act like a rigid string and so the curve preserves the smoothness. If the value of $\beta(s)$ is high the curve is hard and resists to bend, while small values of $\beta(s)$ allows to develop a corner. By adjusting these two coefficients, the curve gets an appropriate elasticity and is able to embrace the object of interest.

2.4.2 Deformable Template

Deformable templates require the prior knowledge about the shape of the object in a direct manner. This priori information is encoded in the form of edge information and this information need not to be exact boundaries of the image. The difference between the snakes and deformable templates is that snakes are form-free energy minimizing functions. In snakes model, there is no global structure of the curve except for some general regularization constraints such as continuity and smoothness of the boundary.

If the objects are corrupted by the noise or degraded in some way so that the original shape is lost then deformed template may match the object better than the snakes model by using an appropriate edge detector. Then all founded objects are matched with the template base and similar objects are checked by aligning the templates

in the data base with the image in question using some potential energy function. This template is the most likely a priori shape of the object. Further, small deformations that leave the template similar to its original shape are more likely than larger displacements. Therefore, we impose a probability distribution on the images in data base to bias the possible deformed templates. By varying the parameters of the distribution, the confidence of prototype templates can be adjusted. In order to project a shape found in an image onto the shape base, we have to extract that shape from the image. For this purpose low-level methods are suitable. So these deformable templates operates on lower level doing the rough part of the work - extracting objects - while the high-level methods are for analyzing the results and making a decision. [5].

2.4.3 Dynamic Contour

Snakes and deformable templates may be labeled as dynamic contours because they show dynamic behavior. Active contours can be applied statically, to single images, or dynamically to image sequences. In dynamical applications, some additional moments may be incorporated in the model to convey any prior knowledge about object motions and deformation. As opposed to snake where only the active contour is varying, in dynamic contours the edge map is varying too and the snake is applied on a sequence of images. The equation of motion for such a system extends from the snake model to a new model with additional terms governing inertia and viscosity. These groups of active contours find their applications in motion tracking, traffic monitoring, visual speech recognition and so on.

2.4.4 Why Level Set?

Shape recovery has always been a critical component in two-dimensional (2-D) and three-dimensional (3-D) medical imagery since it assists largely in medical therapy. The recovery of shapes of the human body is more difficult compared to other imaging fields due to the large variability in shapes and the complexity of medical structures. Deformable models have played a critical role in shape representation and thus become an extremely popular technique in shape recovery. However, there are two main limitations in parametric deformable models. First, in situations where an initial model

and a desired object boundary differ greatly in size and shape, the model must be re-parameterized dynamically to recover the object boundary. The second limitation is its difficulty in dealing with topological adaptation such as splitting or merging model parts. As an alternative, geometric deformable models, or the level set methods, provide an elegant solution to address the primary limitations of parametric ones by embedding propagating interface as the zero level set of a higher dimensional function ϕ while changing its topology. The main characteristic of the level set is its ability to pick up the desired topology of the shape being segmented. Hence, the accuracy of the segmentation process depends on when and where the propagating surface needs to stop. Among the traditional level set techniques without regularizers, stopping force due to gradient-based edge map is one of the key criteria, which will result in boundary leakage when missing part of boundaries or not clear boundary in the medical images. The most reason is that the gradient will never be infinite in a discrete implementation and thereby the front will never fully stop when it reaches an estimated boundary. Thus the curve evolution can't be converged to the real goal boundary exactly.

In the level set method, a continuous function φ is introduced over the whole computational domain. This level set function is given the property of a distance function indicating the shortest distance to the interface and thus, the zero level set of the auxiliary function φ represents the interface. The level set method was first introduced by Osher & Sethian (1988) and later extended to incompressible two-phase flow by Sussman, Smereka & Osher (1994).These notes present a brief introduction to and an overview of the most important aspects of the level set method and incompressible two-phase flow. The major problem of level set segmentation is boundary leakage when a weak boundary or missing part of a boundary occurs. Some efforts, e.g., adding extra stopping criteria or region information, have been used to avoid such problem. However, in existing level-set techniques, the gradient information is used as stopping criteria for curve evolution, and also provides the attracting force to the zero level set from a target boundary.

2.5 Introduction to Level Sets

The level sets aims at finding a minimal length curve that preserves two main properties:

- It is regular and smooth,
- It is attracted by the boundary points (important boundary-based information),

The propagation of curve which is implemented by the level set theory deals automatically the changes of topology (splitting and merging), thereby allowing multiple curves to be the result of the evolution of a single initial curve. Level-set Segmentation methods have drawn specific attention in these past few years. Level-sets are active contours particularly designed to handle the segmentation of deformable structures. They display interesting elastic behaviors, and can handle topological changes. In the level-set formulation however, the boundary of an object is modeled by a deformable curve front whose propagation speed is a function of curvature [6].

2.5.1 Speed Term

In order to make the speed function of the front approach zero in the neighborhood of a desired shape, we employ the following model [6, 7]:

$$v_a = \frac{c}{1+(\nabla G_\sigma * I(X))^k} \tag{2.3}$$

where k is a parameter related to the curvature, $G_\sigma * I$ denotes the image convolved with a Gaussian smoothing filter whose characteristic width σ; X is a point on τ; k is a positive integer.

2.5.2 Level Set Segmentation

As shown by Osher and Sethian , the central idea in the level set segmentation approach is to represent the front $\gamma(t)$ as the level set $\{\phi = 0\}$ of a function ϕ .For a moving closed surface $\gamma(t)$, an Eulerian formulation for the motion of the surface propagating along its normal direction with speed F is defined as:

$$\phi(x, y, t = 0) = \pm d \tag{2.4}$$

Where d is the distance from (x, y) to γ (t), and the plus (minus) sign is chosen if the point (x, y) is outside (inside) the initial surface γ $(t = 0)$. And the evolution equation of level set function for $\phi(x, y, t)$ takes the following formula:

$$\phi_t + F|\nabla\phi| = 0 \tag{2.5}$$

Usually, the speed function F can be written as an explicit level set scheme:

$$F = F_{prop} + F_{curv} + F_{adv} \tag{2.6}$$

Where F_{prop} is the propagation expansion speed, F_{curv} is the dependence of the speed on the curvature k, and F_{adv} is the advection speed. The final equation for the level set segmentation can be rewritten as:

$$\phi_t + g_I(1 - \varepsilon k)|\nabla\phi| - \beta_1 \nabla P.\nabla\phi = 0 \tag{2.7}$$

Where β_1 is the edge strength constant, $(\nabla P.\nabla\phi)$ denotes the projection of an attractive force vector on the normal to the surface, P is realized as the gradient of a potential field which attracts the surface to edges in the images such as [5,6]:

$$P = -|\nabla[G_\sigma * I(x, y)]| \tag{2.8}$$

and g_I is the stopping term based on the image gradient which can be estimated by a convoluted image as:

$$g_I = \frac{1}{1 + |\nabla[G_\sigma * I(x, y)]|} \tag{2.9}$$

The term g_I has the values that are closer to zero in region of high image gradient and values that are closer to unity in the regions with relatively constant intensity, such as in homogeneous regions. In other words, the term is expected to have a sharp change

according to the image gradient and retards the evolving front from passing out of the desired region.

2.5.3 Initialization

The initialization process is a key component in the overall level set segmentation process because any proper initialization of the first particles (and their radii of influence) drives markedly the quality of the convergence towards the boundary of the structure. To set up a robust initialization process, one must rely on easily computable features in the image data like distance of the evolving contour from the actual interface and sign of that distance function according to whether the point on the contour is inside or outside the actual boundary.

2.5.4 Level Set Formulation

For 2D image segmentation, the level set boundary is the zero level set of an implicit function $\phi : R^2 \rightarrow R$. The level set methodology tracks the motion of the zero level set boundaries according to forces acting normally to the zero level set curve. In order to achieve fast processing of the level set propagation, the function φ is defined on a discrete set of points in R^2. The level set equation for front propagation with a 2D speed function, F(x, y), acting normal to the level set curve, is given by the partial differential equation

$$\frac{\partial \phi}{\partial t} + F|\nabla \phi| = 0 \tag{2.10}$$

where $\nabla \phi(x, y)$ is the gradient of ϕ and $|\ |$ is the magnitude operator. The level set evolves according to the speed function F, and it will continue to propagate as long as the speed function is positive. Therefore, when level sets are used for image segmentation, the segmentation problem becomes one of determining the appropriate speed function and initializing the implicit function zero level set points at the seed points. The speed function must be created so that it stops the level set propagation at natural boundaries.

Level set segmentation has retained its attention in the clinical applications due to their topological flexibility and independence of the parameterizations of the evolving contour. However, segmentation process is still a challenge because of the image noise and in homogeneities; therefore segmentation algorithms can not depend only on image information but also have to exploit the prior knowledge of shapes and other properties of the structures to be segmented. The segmentation approach depends on both gray level intensity and shape information; whereas the shape information is gathered from a set of training shapes. A signed distance function is assigned to each shape and the signed distance values are collected in the form of a histogram representing the occurrences of each value. Probability density functions of the object and background are formed based on the signed distance value in addition to the gray level intensity.

2.5.5 Shape Modeling by Level Sets

Shape representation is the main task in shape analysis. The selection of such representation is very important in several medical applications such as registration and segmentation. These are more powerful enough to capture local deformations and they require a large number of parameters to deal with important shape deformations. So an emerging way to represent shapes is derived using the level sets. This representation is invariant to translation and rotation. Given a curve/surface V that represents boundaries of a certain shape; we can define the following level set function:

$$\phi(x,y,z)=\begin{cases}0 & (x,y,z)\in V\\ d((x,y,z),V) & , \ (x,y,z)\in R_V\\ -d((x,y,z),V) & otherwise\end{cases} \tag{2.11}$$

where R_V is the region defined by the shape and $d((x,y,z),V)$ is the minimum Euclidean distance between the image location (x, y, z) and the curve/surface V . By this representation, we can construct a database of curves/surfaces and signed distance functions that represent the variations for certain shape.

2.5.6 Curve/Surface Evolution and Level Sets

Within the level set formalism, the evolving curve/surface is a propagating front embedded as the zero level of a scalar function $\phi(x,y,z,t)$. The continuous change of $\phi(x,y,z,t)$ can be described by the partial differential equation:

$$\frac{\partial\phi(x,y,z,t)}{\partial t}+F(x,y,z)\left|\nabla\phi(x,y,z,t)\right|=0 \tag{2.12}$$

where $F(x, y, z)$ is a velocity function and $\nabla=\left[\frac{\partial}{\partial x},\frac{\partial}{\partial y},\frac{\partial}{\partial z}\right]^T$ the function $\phi(x,y,z,t)$ deforms iteratively according to $F(x, y, z)$, and the position of the 2D/3D front is given at each iteration by solving the equation $\varphi(x, y, z, t) = 0$. Practically, instead of Eq. (2.16), the value $\phi(x,y,z,t_{n+1})$ at step n+1 is computed from $\phi(x,y,z,t_n)$ at step n by the relation given in Eq.(2.13) [8]:

$$\phi(x,y,z,t_{n+1})=\phi(x,y,z,t_n)-\Delta t.F\left|\nabla\phi(x,y,z,t_n)\right| \tag{2.13}$$

The design of the velocity function $F(x,y,z)$ plays the major role in the evolutionary process.

$$F(x,y,z)=v-\varepsilon k(x,y,z) \tag{2.14}$$

where $v = 1$ or -1 for the contracting or expanding front respectively, ε is a smoothing coefficient which is always small with respect to 1, and $k(x,y,z)$ is the local curvature of the front and acts as a regularization term.

2.5.7 Signed Distance Function

Signed distance function is commonly used for level set schemes. During the image segmentation, the level set function can be changed into a non-distance function with the initial level set function defined as a signed distance function and it has to recompute the level set function periodically based on equation (2.15). [9].

$$\frac{\partial \phi_i}{\partial t} = sign(\phi_i)(1 - |\nabla \phi_i|) \tag{2.15}$$

During the positive value of $\frac{\partial \phi}{\partial t}$ the information will go some way and when its negative value the information goes in the other way so it always has positive and negative parts. So by this way the level set function will have a zero level through the segmentation process which means that it's signed distance.

2.5.8. Algorithm

Step 1: Initialize ϕ_i for i =1: K.

Step 2: t = t + 1,

Step 3: Update each function using equation (2.13).

Step 4: Solve equation (2.15) for each iteration.

Step 5: Smooth each function and remove noise.

Step 6: if steady state is not reached, then go to Step 1,

else go to next slice.

Step 1 is very important since had initialization leads to bad segmentation [10]. The role of a level set method for image processing often relates to PDE techniques involving one or more of the following features:

1) Regularization of the solutions,

2) Representing boundaries, and

3) The numerics developed for the level set methods.

2.6 General Concepts of Level set

Boundary value and initial value partial differential equations describe the interface motion of a curve .This curve moves in a direction normal to itself (where the normal direction is oriented with respect to an inside and an outside) with a known speed function F.The motion of this interface in its normal direction depends on speed function which is defined as follows:

$$F = F(L, G, I) \tag{2.16}$$

Where

- L=Local properties are those determined by local geometric information, such as curvature and normal direction.
- G=Global properties of the front are those that depend on the shape and position of the front. For example, the speed might depend on integrals along the front and/or associated differential equations.
- I=Independent properties are those that are independent of the shape of the front, such as an underlying fluid velocity that passively transports the front.

Most of the challenges in the interface problems come from producing an adequate model for the speed function F; Given F and the position of an interface; the objective is to track the evolution of the interface. If F>0, the front always moves "outward" and the position of this expanding front is characterized by the arrival time T(x,y) of the front as it crosses each point(x,y) as shown in figure below [11].

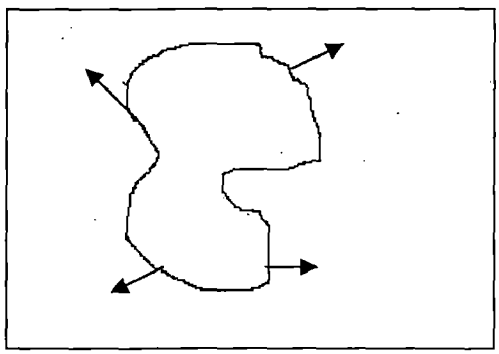

Fig.2.2 The expanding front F>0

The front can move forward and backward, and hence can pass over a point (x, y) several times. Thus, the crossing time T(x, y) is not a single-valued function. So we embed the initial position of the front as the zero level set of a higher-dimensional function ϕ.The evolution of this function ϕ combined with the front through a time-dependent initial value problem. At any time the front is given by the zero level set of the time-dependent level set function.

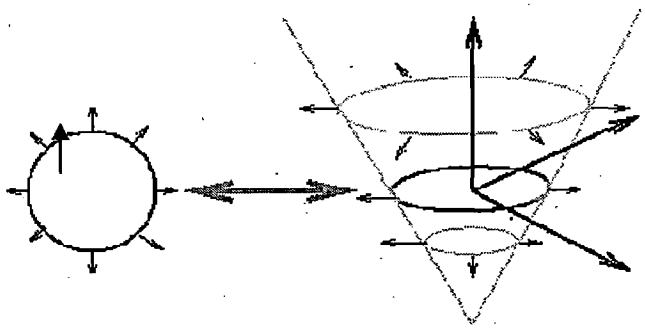

Fig. 2.3: Level Set methodology and curve propagation. The right figure column shows the evolving level set function, while on the right the curve corresponding to the zero level set values of the surface.

The level set value of a particle on the front with path x (t) must always be zero, hence

$$\phi(x(t),t)=0 \tag{2.17}$$

By the chain rule,

$$\phi_t+\nabla\phi(x(t),t).x'(t)=0 \tag{2.18}$$

since F is the speed in the outward normal direction, then x' (t).n=F,

Where $n=\nabla\phi/|\nabla\phi|$

The evolution equation for ϕ, is

$$\phi_t+F|\nabla\phi|=0 \text{ given } \phi(x,t=0) \tag{2.19}$$

This is the level set equation given by Osher and Sethian.

The *advantages* of these level sets are

- Topological change sin the evolving front can handled naturally. The position of the front at time t is given by the zero level set .This set need not be a single curve, and it can be break and merge as t advances.

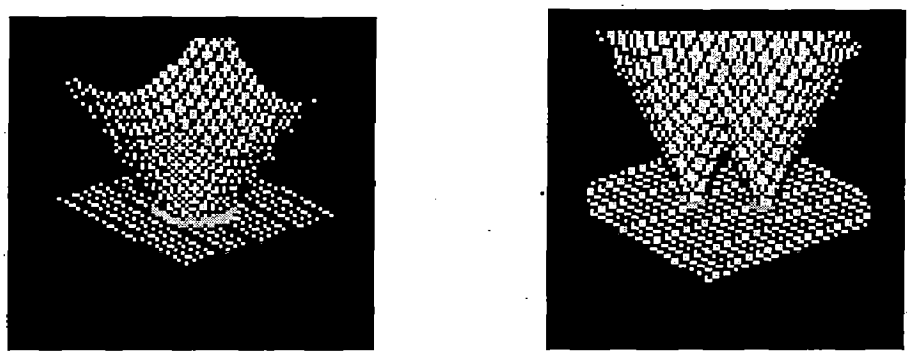

Fig 2.4 Breaking of initial curve as t advances

- It depends on the solutions of the associated partial differential equations in order to guarantee that the unique, entropy-satisfying weak solution,
- Accurately approximated by computational schemes which exploit techniques borrowed from the numerical solutions.
- Intrinsic geometric properties of the front are easily determined. For example, at any point of the front , the normal vector is given by

$$\vec{n} = \frac{\nabla \phi}{|\nabla \phi|} \tag{2.20}$$

and the curvature of the front at any points is easily obtained from the divergence [11] of the unit normal vector to the front,i.e.,

$$k = \nabla . \frac{\nabla \phi}{|\nabla \phi|} = \frac{\phi_{xx}\phi_y{}^2 - 2\phi_x\phi_y\phi_{xy} + \phi_{yy}\phi_x{}^2}{\left(\phi_x{}^2 + \phi_y{}^2\right)^{3/2}} \tag{2.21}$$

CHAPTER 3
RANDOMIZED HOUGH TRANSFORM

This chapter presents a novel variational method called Randomized Hough Transform to extract the ellipses in ultrasound medical images depending on some statistical and mathematical equations and probabilistic characteristics which is going to be used as initial curve in fetal head detection. This chapter discusses the basic concepts and limitations of Hough Transform and advantages of Randomized Hough Transform over the Hough Transform.

3.1 Introduction

Randomized Hough Transform (RHT) has been recently proposed as a new and efficient transform for curve detection. The RHT was originally proposed by Lei Xu. and they implemented it as a series of random trials rather than taking a single point and computing all the possible shapes that could result from that point, the algorithm takes a set of points sampled randomly from the input set and computes a single parameter-space point [12]. The RHT starts with an empty accumulator. In the case of ellipse, five pixels are chosen randomly from the input and the unique ellipse that these points define is mapped to the parameter-space. This process continues until some threshold is reached in accumulator and an ellipse is determined. The algorithm stops when no ellipses are detected for a preset number of iterations or a predefined number of samples.

The RHT is more difficult to apply to circle and ellipse detection. Solving the equation of an ellipse for five sampled points is difficult because the equation is non-linear with respect to the parameters (center, rotation of ellipse and axes). Finding the solution requires solving a set of five non-linear equations. The algorithm has good computational speed and small storage requirements due to random sampling and correct and more accurate detections, especially in noisy images.

3.2 Hough Transform

Hough Transform (HT) was proposed first by Hough in 1962, to detect lines and other shapes. Ellipse detection is a key problem in digital image processing. In order to detect circles, ellipses and even irregular objects effectively and quickly by using the Hough transform, many variations have been suggested.Jeng and Tsai suggested a two-stage GHT, generalized Hough transform [16].They used half-lines and circles to replace the displacement vectors in evaluating the different parameters to identify the object. To reduce the problems such as large memory requirement and heavy computation for identifying non analytic objects, Xu proposed (RHT).In comparison with HT and its variants; RHT has advantages of fast speed, small storage and high parameter resolution [20].

The Hough Transform (HT) is a well known technique for detecting parametric curves in images and it becomes a popular method to extract image features like straight lines or circles and has been generalized to extract any arbitrary shape at a given orientation and a given scale. Hough transform converts the spatial data from an image space into the parameter space. Owing to its robustness to noise and inexact data, the HT is a very attractive approach for object recognition applications. However, the HT algorithms suffer from two major difficulties. The first one is its huge computational complexity and the second one is its huge memory consumption.

The Randomized Hough Transform (RHT) has been proposed recently as an efficient version of HT that reduces the time requirements significantly. Instead of transforming every contour pixel into higher dimensional hyper surface in the parameter space of HT, the RHT randomly selects p contour pixels of an image and maps them onto a certain point of the parameter space. For example in the case of straight line detection, two contour pixels from the original binary edge image are transformed into a point in the two dimensional parameter space. Such pixel pairs are randomly selected, the parameter point is found from the straight line equation and a unit is added to the corresponding cell of the accumulator array [17].

The Hough transform is a standard technique for detecting curves. It consists of three steps:

1. A pixel in the image is transformed into a parameterized curve.
2. Valid curve's parameters are binned into an accumulator where the number of curves in a bin equals to its score.
3. A curve with a maximum score is selected from the accumulator to represent a curve in the image.

This basic Hough transform suffers many difficulties stemming from binning the curves (large accumulators and much processing time). To reduce these problems, Lei Xu proposed a Randomized Hough Transform (RHT).

3.3 Why Randomized Hough Transform?

The Hough transform (HT) is a standard technique for detecting curves. The HT consists of three steps:

1. A pixel in the image is transformed into a parameterized curve,
2. Valid curve's parameters are binned into an accumulator where the number of curves in a bin equals its score, and
3. A curve with a maximum score is selected from the accumulator to represent a curve in the image.

This basic Hough Transform suffers from many difficulties stemming from binning the curves. The accumulator's bin sizes are determined by"windowing and sampling the parameter space in a heuristic way". To detect curves in a variety of images the window size must be large, and to detect curves with a high accuracy there must be a high parameter resolution. These two properties require a large accumulator and much processing time. Xu et. al. identified the following possible problems that can occur if the accumulator is not properly defined. These are [13]:

1. Failure to detect some specific curves.
2. Difficulties in finding local maxima

3. Low accuracy
4. Large storage and
5. Low speed

To reduce these problems Xu proposed a RHT which selects *n* pixels randomly from an image and fits them to a parameterized curve. If the pixels fit within a tolerance they are added to an accumulator with a score. Once a specified number of pixel sets are selected the curves with the best score are selected from the accumulator and its parameters are used to represent a curve in the image and due to selection of small random subset of pixels, *n* this method reduces the storage requirements and computational time needed to detect curves in an image.

3.4 **Randomized Hough Transform**

The RHT randomly selects n pixels from the image and fits them to a parameterized curve. If the pixels fit within a tolerance they are added to an accumulator with a score. Once a specified number of pixel sets are selected the curve with the best score is selected from the accumulator and its parameters are used to represent a curve in the image .This method reduce the storage requirements and computational time needed to detect curves in an image [18].

The RHT is based on probabilistic method and due to sampling a small subset of points is examined thus the computation time and storage is reduced. It guarantees infinite and continuous parameter space. Current versions of RHT work only on binary images so that a preparation step of threshold or filtering has to be applied to grayscale images beforehand.

We present a new approach for the segmentation of fetal head in 2D image data. Our algorithm, which requires only a few initial values and minimal user interaction, can be used to initialize complex deformable models and is based on RHT [19]. The Hough transform is a well-known method for robust parametric object detection, where feature pixels such as edges in the input image are mapped to a discrete parameter space, whose maxima denote the required object. In order to detect ellipses or straight elliptical cylinders, which have a relatively large number of parameters (leading

to excessive space/time complexity for the conventional Hough transform) the RHT will used.

The RHT uses a randomly chosen subset of the input data, together with a many-to-one sampling scheme that maps input point sets to a small number of points in the parameter space. Usually, this means that a point set sufficient to uniquely determine the parametric object at hand is mapped onto a single parameter vector, which is in contrast to the conventional Hough transform. This allows using space-efficient dynamic accumulator schemes. Together with random sampling, the advantage is that parameter spaces of higher dimensions remain tractable. The drawbacks which are inherent to coarse to fine and parameter-space decomposition Hough transforms, such as increased noise sensitivity and projection artifacts can be alleviated by the RHT, because the parameter space can always have both full dimension and parameter resolution.

3.4.1 Object Parameterizations for Ellipses

To detect ellipses in 2D slices of elliptical generalized cylinders, we apply an ellipse parameterization proposed for the Hough transform. Given five coplanar points, this approach determines the unique ellipse (if there is any) that passes through them. Let

$$\begin{aligned} U &= \cos(2\theta)\frac{1-e^2}{1+e^2} \\ V &= \sin(2\theta)\frac{1-e^2}{1+e^2} \\ R &= 2x_c(1-U)-2y_cV \\ S &= 2y_c(1+U)-2x_cV \\ T &= \frac{2a^2b^2}{a^2+b^2}-\frac{x_cR}{2}-\frac{y_cS}{2} \\ e &= \frac{b}{a} \end{aligned} \tag{3.1}$$

with (x_c, y_c)being the center, a and b are semi axes and θ is the rotation angle of the ellipse. Then the algebraic variety given by

$$x^2+y^2+U(y^2-x^2)-2Vxy-Rx-Sy-T=0 \tag{3.2}$$

yields the ellipse. To determine U, V, R, S, T, substituting five distinct points into Eq. (3.2) results in a system of five linear equations. The result is then used to solve Eq. (3.1) for the natural ellipse parameters (x_c, y_c), a, b and θ . Thus, the feature space for this ellipse parameterization is a subset of the $\Re^5$, where samples of five points are used [23].

When using random sampling schemes for RHT, it is normally no longer necessary to consider all feature points of the input data set. Usually, a subset whose size depends on the quality of the input data is used. This subset is typically generated by drawing a sample of a given size from the input data points [24].

3.4.2 Ellipse Detection Using RHT

An ellipse with semi axes a, b and center (X, Y) can be described with the parametric equations:

$$x = X + a\cos\theta \tag{3.3}$$
$$y = Y + b\sin\theta$$

When the angle θ sweeps through the full 360 degree range, the points (X, Y) trace the perimeter of a circle.

3.5 Algorithm

This algorithm executes for a number of epochs, where an epoch is the processing that occurs to find ellipses through accumulation. The algorithm completes when the maximum number of epochs is reached or it does not find ellipses for a specified number of epochs. The main body of processing occurs in the for loop where ellipses found are accumulated and scores are given to that ellipses. The larger the number of iterations the more likely multiple similar ellipses will be accumulated into a single ellipse and gives a higher score. At the end of the for loop the accumulator is searched for ellipses with high scores, which are placed in a best ellipse table [15]. The conventional Randomized Hough transform is a many to one (m->1) algorithm in which pairs of points are randomly selected and fitted to a parameterized curve. The algorithm

is basically a stochastic process, which means that the outcome doesn't have to be the same each time.

1. Initialize the number of samples and region of interest.
2. Count the nonzero pixels and select any 5 points (p1, p2, p3, p4, p5) of them.
3. With the help of these 5 points the following stable and parametrically linear model (Leavers 1992) is solved to get U, V, R, S, T.

$$x^2 + y^2 - U\left(x^2 - y^2\right) - V2xy - Rx - Sy - T = 0 \tag{3.4}$$

$$A = \begin{bmatrix} x_1^2 - y_1^2 & 2x_1y_1 & x_1 & y_1 & 1 \\ x_2^2 - y_2^2 & 2x_2y_2 & x_2 & y_2 & 1 \\ x_3^2 - y_3^2 & 2x_3y_3 & x_3 & y_3 & 1 \\ x_4^2 - y_4^2 & 2x_4y_4 & x_4 & y_4 & 1 \\ x_5^2 - y_5^2 & 2x_5y_5 & x_5 & y_5 & 1 \end{bmatrix}$$

$$B = \begin{bmatrix} x_1^2 + y_1^2 \\ x_2^2 + y_2^2 \\ x_3^2 + y_3^2 \\ x_4^2 + y_4^2 \\ x_5^2 + y_5^2 \end{bmatrix} \qquad X = \begin{bmatrix} U \\ V \\ R \\ S \\ T \end{bmatrix} \tag{3.5}$$

X=A/B

4. Now compute the parameters A, B, C, D, E and F of the basic quadratic equation

$$Ax^2 + Bxy + Cy^2 + Dx + Ey + F = 0 \tag{3.6}$$

If there doesn't exist a solution, go to 1).

5. Check the inequality $b^2 - 4ac < 0$, which has to be true for a valid ellipse. If false, go to 1).

6. Now compute the natural parameters i.e. center (x_0, y_0) and semi major and semi minor axes a and b and angle of rotation ϕ are found by comparing (3.4) with the following equation. Those parameters satisfy the equation:

$$\frac{((y-y_0).\sin\theta+(x-x_0).\cos\theta)^2}{a^2}+\frac{((y-y_0).\cos\theta-(x-x_0).\sin\theta)^2}{b^2}=1 \qquad (3.7)$$

7. Check for the validity of ellipse i.e. $x_0 and y_0$, a and b are positive, $x_0 and y_0$ are not larger than image width and height, respectively; a is greater than b; and a and b are not larger than half of the diagonal length of the image.

8. Now search the list of already found parameter sets. If there is a parameter set whose values are close to the one newly found (determined by an epsilon) increase the count of this parameter set. Each parameter set has a so called count value, which tells how many times these same parameters have been found. If there is no similar set, simply add the new parameter set to the list and set its count to 1.

9. Increment samples and check for number of samples reached are not.

10. After a specified amount of those parameter sets is found (so called epoch), analyze the list (or matrix) of parameter sets. Take every set that having maximum count value and find corresponding parameters $para_{est}$.

11. Check for convergence of ellipse i.e. the change in $para_{est}$ from the previous iteration is small(less than 2.5^0 in ϕ , less than two pixels in any of (x_0, y_0), a, b and less than 6 pixels total in (x_0, y_0), a, b.

12. If there were some ellipses found satisfying the above convergence criteria, then draw the corresponding ellipse else clear the list of parameter sets and starts with another epoch. (i.e. go to 1)).

It should be clear that there are many parameters in this algorithm that have an impact on the performance. Epoch the number of loops done before parameter data is analyzed convergence criteria to consider an ellipse in the image as existent [25].The flowchart of this algorithm is shown in section 3.7.

3.6 Verifying the Ellipses Existing in the Image

Even though at this point the ellipse parameters (p, q, a, b, c) were found it is possible the ellipse does not exist in the image. Two checks occur to verify the ellipse exists. First, because the ellipse is defined by the general equation for a conic section [14]:

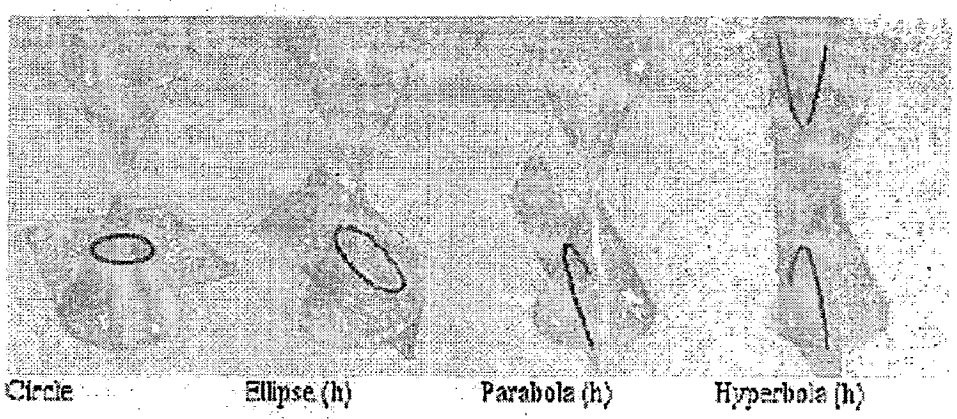

Fig 3.1: Example of different two-dimensional shapes derived from passing a plane through a conic section.

$$ax^2 + bxy + cy^2 + dx + ey + f = 0 \tag{3.8}$$

The sign of $b2$ -4ac determines the type of conic section:

< 0 Ellipse or Circle

$= 0$ Parabola

> 0 Hyperbola

If the sign is negative then it is an ellipse. The ellipse's parameters were found and the ellipse points are generated by solving the following equations for theta = 0 *to* 2 Π:

$$x = a \cos(\text{theta})$$

$$y = b \sin(\text{theta}) \tag{3.9}$$

3.7 Flowchart of Randomized Hough Transform

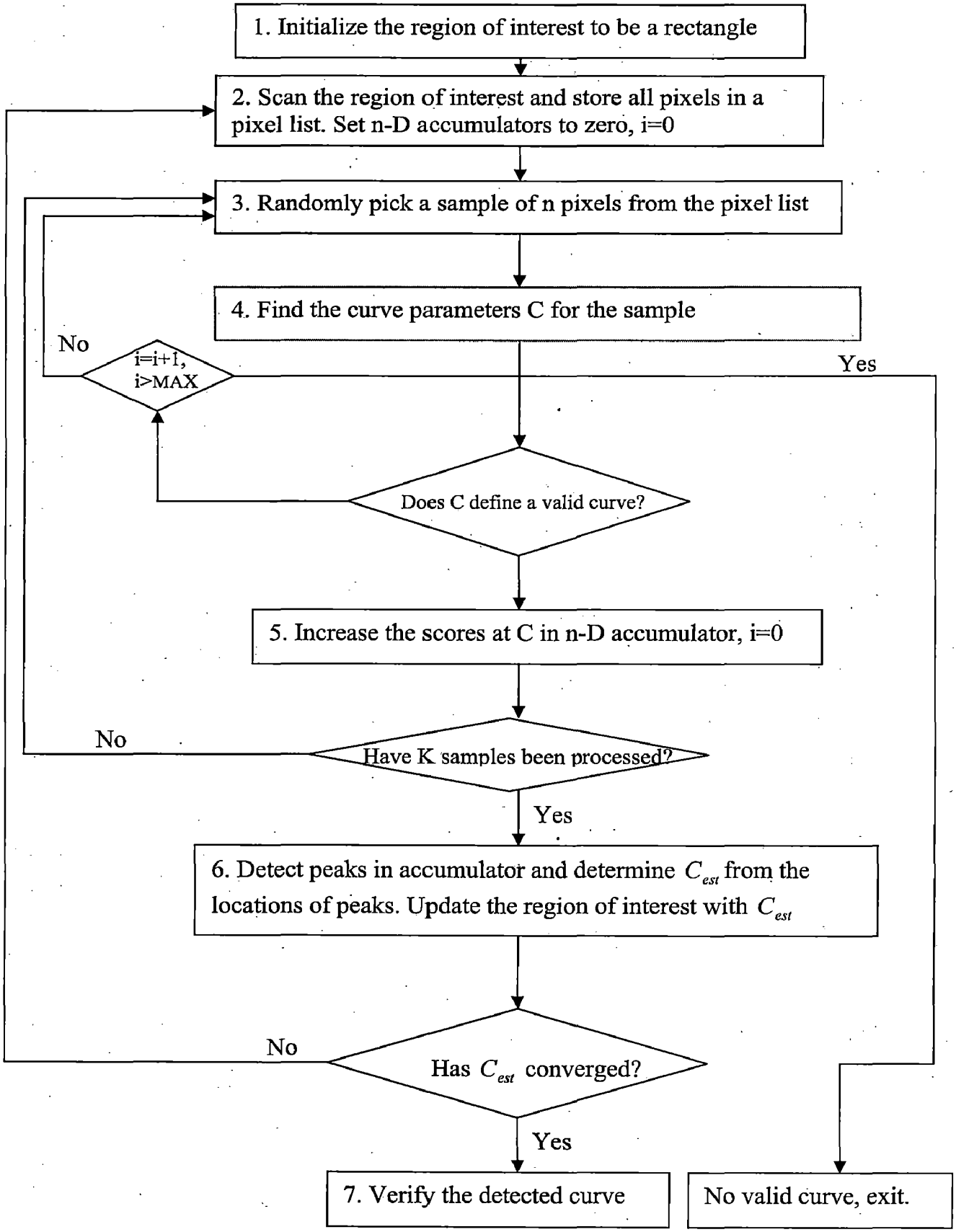

Fig 3.2 Flow diagram of randomized Hough transform (RHT) for ellipse detection

CHAPTER 4
IMAGE SEGMENTATION

This chapter presents a novel variational method for image segmentation that unifies some morphological operators to enhance the image and Randomized Hough Transform Which was already discussed in previous chapter to initialize the required contour for segmentation of medical images which is necessary step for level set method in detecting the fetal head from ultrasound images.

According to the motion equations, initial curve is propagated towards the segmentation result under the influence of boundary and region-based forces, and being constrained by a regularity force. The changes of topology are naturally handled thanks to the level set implementation; the performance of this method is demonstrated on a variety of ultrasound images.

Segmentation of medical images is a challenging problem due to the complexity of the images, and the lack of anatomical models that fully capture all possible shape variations for each structure. Recently, level set methods have been applied to the problems that arise in geometry, fluid mechanics, computer vision, manufacturing processes, and medical imaging. The level set method is essentially a moving interface problem. It embeds the interface as the level set of a higher dimensional function, such as the signed distance to the interface. The main advantage of the level set method over other numerical methods for establishing an interface is its natural treatment of topological changes such as merging and breaking. These changes can be difficult to handle with methods based on parameterization.

4.1 Pre-processing Stage

One of the major drawbacks of ultrasound images is the presence of speckle noise. Such noise degrades the quality of the ultrasound images and hence, influences the accuracy of any segmentation schemes. Thus, it is crucial to utilize an efficient noise removal scheme to reduce this noise. The objective of this stage is to improve the quality of the ultrasound image to achieve better segmentation results. This

stage is completely isolated from the rest of the system. Thus, it can be replaced by any image enhancement stage without affecting the overall system flow. In the proposed scheme, the pre-processing stage consists of three steps. The first and second steps include some morphological operators on the original image and the third step involves skeleton of image [1].

4.1.1 Morphology

Morphological image processing is a set-theoretical approach to image analysis based on shape. The most basic building blocks for many morphological operators are erosion and dilation. In binary images, dilation, in general, causes objects to dilate or grow in size; thus potentially filling-in small holes and connecting disjoint objects. On the other hand, erosion causes objects to shrink. The amount and the way that objects grow or shrink depend upon the choice of the structuring element [21]. Fig 4.1 and Fig 4.2 shows the dilation and erosion of the object A using a circular-shape structuring element B, respectively.

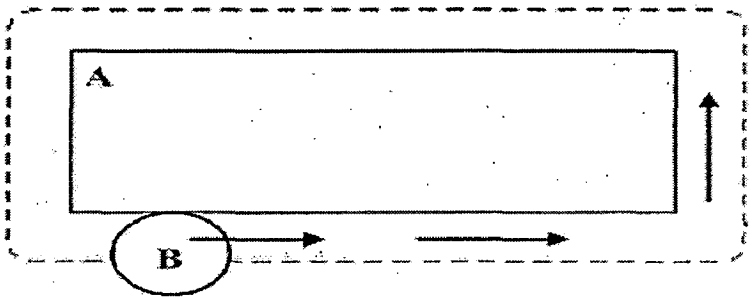

Fig 4.1: The dilation of A by the structuring element B and the result is shown with the dotted line

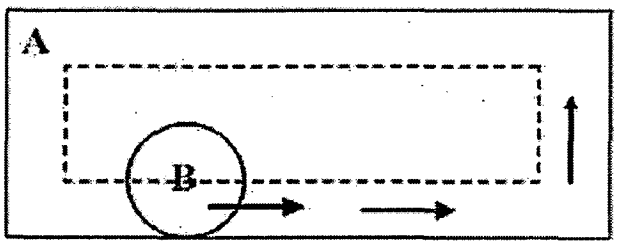

Fig 4.2: the erosion of A by the structuring element B and the result is shown with the dotted line

In grayscale dilation, a structuring element is scanned over the image and point-by-point maximum of the image pixels is computed at each position under the structuring element. This maximum value is the destination pixel value at the location under the center of the structuring element. Grayscale erosion is the dual of grayscale dilation where the maximum is replaced by the minimum operation.

4.1.2 Opening and Closing

Opening generally smoothes the contour of an object, breaks narrow isthmuses, and eliminates thin protrusions. Closing also tends to smooth sections of contours but, as opposed to opening it generally fuses narrow breaks and long thin gulfs, eliminates small holes, and fills gaps in the contour [1].

The opening of set A by structuring element B, denoted $A \circ B$, is defined as

$$A \circ B = (A \ominus B) \oplus B \tag{4.1}$$

Thus, the opening A by B is the erosion of the A by B, followed by a dilation of the result by B.

Similarly, the closing of set A by structuring element B, denoted $A \bullet B$, is defined as

$$A \bullet B = (A \oplus B) \ominus B \tag{4.2}$$

A morphologic binary area opening operation is used to remove small bright objects and closing is used to smooth the boundaries of large bright objects.

The opening operation satisfies the following properties:

i. $A \circ B$ is a subset (sub image) of A.

ii. If C is a subset of D, then $C \circ B$ is a subset of $D \circ B$.

iii. $(A \circ B) \circ B = A \circ B$

Similarly the closing operation satisfies the following properties:

i. A is a subset (sub image) of $A \bullet B$.

ii. If C is a subset of D,then $C \bullet B$ is a subset of $D \bullet B$

iii. $(A \bullet B) \bullet B = A \bullet B$

In both cases the condition iii. indicates that multiple openings or closings of a set have no effect after the operator has been applied once.

4.1.3 Skeleton

It reduces the representation of a structural shape of a plane region in to a graph. This reduction may be accomplished by obtaining the skeleton of the region via a thinning (also called skeletonizing) algorithm. The skeleton of a region may be defined via the medial axis transformation (MAT). The medial axis transformation of a region R with border b is as follows. For each point p in R, find its closest neighbor in b.If p has more than one such neighbor, it is said to belong to the medial axis (skeleton) of R. Thus the skeleton image provided a simple representation of the skull segments and was used for required applications.

4.2 Active Contours without Edges

The classical active contour model uses an edge indicator depending on the image μ_0 to stop the evolving curve on the boundary of the desired object. First define the evolving curve C in Ω, as the boundary of an open subset ω of Ω where inside(C) denotes the region ω, and outside (C) denotes the region $\Omega \setminus \bar{\omega}$. Assume that the image is formed by two regions of approximatively piecewise-constant intensities, of distinct values $\mu_0{}^{i}$ and $\mu_0{}^{0}$. Assume further that the object to be detected is represented by the region with the value $\mu_0{}^{i}$ and C_0 denotes its boundary. Let us consider the following "fitting" term [26]

$$F_1(C) + F_2(C) = \int_{inside(C)} |\mu_0(x,y) - c_1|^2 \, dxdy + \int_{outside(C)} |\mu_0(x,y) - c_2|^2 \, dxdy \qquad (4.3)$$

Where C is any other variable curve, and the constants c_1, c_2 depending on C, are the averages of μ_0 inside and outside C respectively. The above fitting term can be minimized by adding some regularizing terms, like the length of the curve C , and (or) the area of the region inside C .Now the energy functional can be defined as

$$\begin{aligned} F(c_1, c_2, C) &= \mu.Length(C) + \nu.Area(inside(C)) \\ &+ \lambda_1 \int_{inside(C)} |\mu_0(x,y) - c_1|^2 dxdy \\ &+ \lambda_2 \int_{outside(C)} |\mu_0(x,y) - c_2|^2 dxdy \end{aligned} \tag{4.4}$$

Where $\mu \geq 0, \nu \geq 0, \lambda_1, \lambda_2 > 0$ are fixed parameters. In almost all numerical calculations the values are fixed as $\lambda_1 = \lambda_2 = 1$ and $\nu = 0$.

4.2.1 Relation with the Mumford–Shah Function

The Mumford–Shah functional for segmentation is

$$\begin{aligned} F^{MS}(\mu, C) &= \mu.Length(C) \\ &+ \lambda \int_{\Omega} |\mu_0(x,y) - \mu(x,y)|^2 dxdy \\ &+ \lambda \int_{\Omega \setminus C} |\nabla \mu(x,y)|^2 dxdy \end{aligned} \tag{4.5}$$

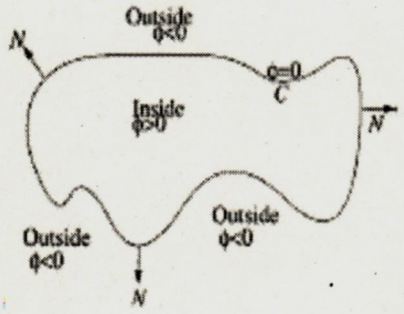

Fig.4.3 Curve C propagating in normal direction.

Where u_0 is a given image, μ and λ are positive parameters. The solution image obtained by minimizing this functional is formed by smooth regions R_i and with sharp

boundaries, denoted as C. A reduced form of this problem is simply the restriction of F^{MS} to piecewise constant functions μ, i.e., $\mu =$ constant c_i on each connected component R_i of $\Omega \setminus C$. It was also pointed out earlier by D. Mumford and J. Shah, $c_i = \text{average}(\mu_0)$ on each connected component R_i. The reduced case is called the minimal partition problem.

Our active contour model with $\nu = 0$ and $\lambda_1 = \lambda_2 = \lambda$ is a particular case of the minimal partition problem, in which we look for the best approximation μ of μ_0, as a function taking only two values, namely

$$\mu = \begin{cases} average(\mu_0) inside C \\ average(\mu_0) outside C \end{cases} \tag{4.6}$$

and with one edge C, represented by the snake or the active contour. This particular case of the minimal partition problem can be formulated and solved using the level set method which is presented in the next section [27].

4.2.2 Level Set Formulation of the Model

The Heaviside function H, and the one-dimensional Dirac measure δ_0, are defined as [28]

$$H(z) = \begin{cases} 1 \ if z \geq 0, \\ 0 \ if z < 0, \end{cases}$$

$$\delta_0(z) = \frac{d}{dz} H(z) \tag{4.7}$$

The energy terms in (4.4) are defined as follows

$$Length\{\phi = 0\} = \int_{\Omega} |\nabla H(\phi(x,y))| dxdy$$

$$= \int_{\Omega} \delta_0(\phi(x,y)) |\nabla \phi(x,y)| dxdy$$

$$Area\{\phi \geq 0\} = \int_{\Omega} H(\phi(x,y)) dxdy \quad ,$$

and

$$\int_{\phi>0}|\mu_0(x,y)-c_1|^2\,dxdy$$

$$=\int_{\Omega}|\mu_0(x,y)-c_1|^2 H(\phi(x,y))dxdy$$

$$\int_{\phi<0}|\mu_0(x,y)-c_2|^2\,dxdy$$

$$=\int_{\Omega}|\mu_0(x,y)-c_1|^2 (1-H(\phi(x,y)))dxdy \tag{4.8}$$

Then, the energy $F(c_1,c_2,\phi)$ can be written as

$$\begin{aligned}F(c_1,c_2,\phi)=&\mu\int_{\Omega}\delta(\phi(x,y))|\nabla\phi(x,y)|dxdy\\&+\nu\int_{\Omega}H(\phi(x,y))dxdy\\&+\lambda_1\int_{\Omega}|\mu_0(x,y)-c_1|^2 H(\phi(x,y))dxdy\\&+\lambda_2\int_{\Omega}|\mu_0(x,y)-c_2|^2 (1-H(\phi(x,y)))dxdy\end{aligned} \tag{4.9}$$

as defined in (4.6), the solution of our model is a particular case of the Mumford–Shah minimal partition problem, and can simply be written using the level set formulation as [29]

$$\mu(x,y)=c_1H(\phi(x,y))+c_2(1-H(\phi(x,y))),(x,y)\in\bar{\Omega} \tag{4.10}$$

Keeping ϕ fixed and minimizing the energy $F(c_1,c_2,\phi)$ with respect to the constants c_1 and c_2, which can be expressed as follows,

$$c_1(\phi)=\frac{\int_{\Omega}\mu_0(x,y)H(\phi(x,y))dxdy}{\int_{\Omega}H(\phi(x,y))dxdy} \tag{4.11}$$

if $\int_{\Omega} H(\phi(x,y))dxdy > 0$ (i.e. if the curve has a non empty interior in Ω), and

$$c_2(\phi) = \frac{\int_{\Omega} \mu_0(x,y)(1-H(\phi(x,y)))dxdy}{\int_{\Omega}(1-H(\phi(x,y)))dxdy} \tag{4.12}$$

if $\int_{\Omega}(1-H(\phi(x,y)))dxdy > 0$ (i.e. if the curve has a non empty exterior in Ω). Then the values of c_1 and c_2 are written as

$$\begin{cases} c_1(\phi) = average(\mu_0) in\{\phi \geq 0\} \\ c_2(\phi) = average(\mu_0) in\{\phi < 0\} \end{cases} \tag{4.13}$$

The associated Euler–Lagrange equation for the unknown function ϕ , we consider slightly regularized versions of the functions H and δ_0 , denoted by H_ε and δ_ε. Thus the associated regularized functional, is defined by [30]

$$\begin{aligned} F_\varepsilon(c_1,c_2,\phi) = {} & \mu \int_{\Omega} \delta_\varepsilon(\phi(x,y))|\nabla\phi(x,y)|dxdy \\ & + \nu \int_{\Omega} H_\varepsilon(\phi(x,y))dxdy \\ & + \lambda_1 \int_{\Omega} |\mu_0(x,y) - c_1|^2 H_\varepsilon(\phi(x,y))dxdy \\ & + \lambda_2 \int_{\Omega} |\mu_0(x,y) - c_2|^2 (1-H_\varepsilon(\phi(x,y)))dxdy \end{aligned} \tag{4.14}$$

Keeping c_1 and c_2 fixed, and minimizing F_ε with respect to ϕ , the associated Euler-Lagrange equation for ϕ can be deduced as follows

$$\begin{aligned} \frac{\partial\phi}{\partial t} &= \delta_\varepsilon(\phi)\left[\mu div\left(\frac{\nabla\phi}{|\nabla\phi|}\right) - \nu - \lambda_1(\mu_0 - c_1)^2 + \lambda_2(\mu_0 - c_2)^2\right] \\ &= 0 in(0,\infty)\times\Omega, \\ \phi(0,x,y) &= \phi_0(x,y) in\Omega \end{aligned} \tag{4.15}$$

4.2.3 Numerical Approximation of the Model

The regularization of H, as proposed in [26], is

$$H_{1,\varepsilon}(z)=\begin{cases}1 if z>\varepsilon\\ 0 if z<-\varepsilon\\ \frac{1}{2}\left[1+\frac{z}{\varepsilon}+\frac{1}{\pi}\sin\left(\frac{\pi z}{\varepsilon}\right)\right] if |z|\le\varepsilon\end{cases} \tag{4.16}$$

The following regularization of H used in my experiments

$$H_{2,\varepsilon}(z)=\frac{1}{2}\left(1+\frac{2}{\pi}\arctan\left(\frac{z}{\varepsilon}\right)\right) \tag{4.17}$$

These distinct approximations and regularizations of the functions H and δ_0 (taking $\delta_\varepsilon = H_\varepsilon{}'$) are presented as shown in figure below [26].

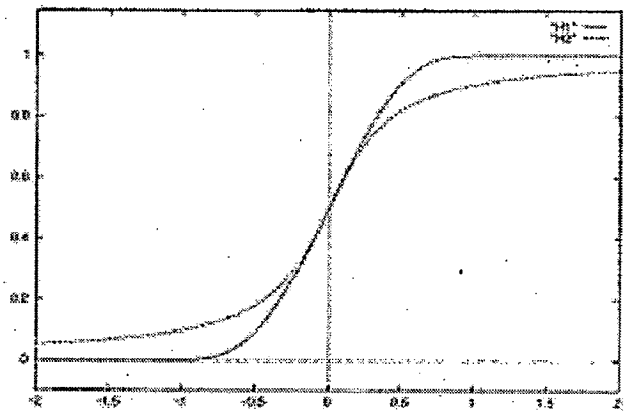

Figure 4.4 Heaviside function

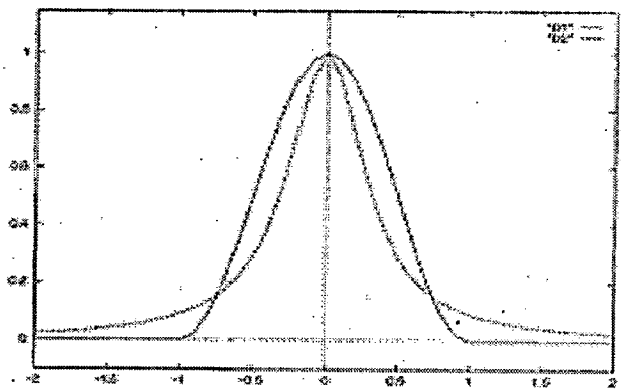

Figure 4.5 Delta function

To discretize the equation in ϕ , we use a finite differences implicit scheme. Let h be the space step, Δt be the time step, and $(x_i, y_j) = (ih, jh)$ be the grid points, for $1 \le i, j \le M$. Let $\phi_{i,j}^n = \phi(n\Delta t, x_i, y_j)$ be an approximation of $\phi(t,x,y)$, with $n \ge 0, \phi^0 = \phi_0$. The finite differences are

$$\begin{aligned} \Delta_-^x \phi_{i,j} &= \phi_{i,j} - \phi_{i-1,j}, & \Delta_+^x \phi_{i,j} &= \phi_{i+1,j} - \phi_{i,j}, \\ \Delta_-^y \phi_{i,j} &= \phi_{i,j} - \phi_{i,j-1}, & \Delta_+^y \phi_{i,j} &= \phi_{i,j+1} - \phi_{i,j}, \end{aligned} \tag{4.18}$$

The algorithm is as follows: knowing ϕ^n , we first compute $c_1(\phi^n)$ and $c_2(\phi^n)$ using (4.11) and (4.12) respectively. Then, we compute ϕ^{n+1} by the following discretization and linearization of (4.15) in ϕ

$$\begin{aligned} \frac{\phi_{i,j}^{n+1} - \phi_{i,j}^n}{\Delta t} = \; & \delta_h(\phi_{i,j}^n)\Bigg[\frac{\mu}{h^2}\Delta_-^x \cdot \left(\frac{\Delta_+^x \phi_{i,j}^{n+1}}{\sqrt{(\Delta_+^x \phi_{i,j}^n)^2/(h^2) + (\phi_{i,j+1}^n - \phi_{i,j-1}^n)^2/(2h)^2}}\right) \\ & + \frac{\mu}{h^2}\Delta_-^y \cdot \left(\frac{\Delta_+^y \phi_{i,j}^{n+1}}{\sqrt{(\phi_{i+1,j}^n - \phi_{i-1,j}^n)^2/(2h)^2 + (\Delta_+^y \phi_{i,j}^n)^2/(h^2)}}\right) \\ & - v - \lambda_1(\mu_{0,i,j} - c_1(\phi^n))^2 + \lambda_2(\mu_{0.i.j} - c_2(\phi^n))^2\Bigg] \end{aligned} \tag{4.19}$$

This linear system is solved by an iterative method. For this algorithm reinitialization of level set function ϕ is done by using the following equation

$$\frac{\partial \phi}{\partial t} = sign(\phi_0)(1 - |\nabla \phi|) \tag{4.20}$$

Re-initialization has been extensively used as a numerical remedy in traditional level set methods. The standard re-initialization method is to solve the above reinitialization where ϕ_0 is the function to be re-initialized, and $sign(\phi)$ is the sign function. If ϕ_0 is not smooth or ϕ_0 is much steeper on one side of the interface than the other, the zero level set of the resulting function ϕ can be moved incorrectly from that of the original function . When the level set function is far away from a signed distance function, these methods may not be able to re-initialize the level set function to a signed distance function. The evolving level set function can deviate greatly from its value in a small number of iteration steps, especially when the time step is not chosen small enough and the re-initialization process is quite complicated, expensive, and have subtle side effects.

4.2.4 Algorithm

Finally, the principal steps of the algorithm are:

1. Initialize ϕ^0 by ϕ_0 .
2. Compute $c_1(\phi^n)$ and $c_2(\phi^n)$ by (4.11) and (4.12).
3. Solve the PDE in ϕ from (4.15), to obtain ϕ^{n+1} .
4. Reinitialize ϕ locally to the signed distance function to the curve.
5. Check whether the solution is stationary. If not, $n = n+1$ and repeat.

We note that the use of a time-dependent PDE for ϕ is not crucial. The stationary problem obtained directly from the minimization problem could also be solved numerically, using finite differences scheme.

4.3 Segmentation using Level Set Evolution without Re-initialization

In this method geometric active contours forces the level set function close to a signed distance function, and therefore completely eliminates the need of the costly re-initialization procedure. This variational formulation consists of an internal energy term that penalizes the deviation of the level set function from a signed distance function, and an external energy term that drives the motion of the zero level set toward the desired image features, such as object boundaries. The resulting evolution of the level set

function is the gradient flow that minimizes the overall energy functional. The proposed variational level set formulation has three main advantages over the traditional level set formulations. First, a significantly larger time step can be used for numerically solving the evolution partial differential equation, and therefore speeds up the curve evolution. Second, the level set function can be initialized with general functions that are more efficient to construct and easier to use in practice than the widely used signed distance function. Third, the level set evolution in our formulation can be easily implemented by simple finite difference scheme and is computationally more efficient. The following sections describe our method and its implementation [31].

4.3.1 General Variational Level Set Formulation with Penalizing Energy

It is crucial to keep evolving level set function as an approximate signed distance function during the evolution, especially in a neighborhood around the zero level set. It is well known that a signed distance function must satisfy a desirable property of $|\nabla\Phi| = 1$. Conversely, any function Φ satisfying $|\nabla\Phi| = 1$ is the signed distance function plus a constant. The following integral is a metric to characterize how close a function Φ is to a signed distance function in $\Omega \subset R^2$. This metric will play a key role in our variational level set formulation.

$$\rho(\phi) = \int_{\Omega} \frac{1}{2}(|\nabla\Phi| - 1)^2 \, dxdy \tag{4.21}$$

$$\varepsilon(\phi) = \mu\rho(\phi) + \varepsilon_m(\phi) \tag{4.22}$$

where $\mu > 0$ is a parameter controlling the effect of penalizing the deviation of Φ from a signed distance function, and $\varepsilon_m(\phi)$ is a certain energy that would drive the motion of the zero level curve of Φ.The Gateaux derivative (or first variation) of the functional ε i.e. $\frac{\partial\varepsilon}{\partial\phi}$ is the gradient flow that minimizes the functional ε is

$$\frac{\partial\phi}{\partial t} = -\frac{\partial\varepsilon}{\partial\phi} \tag{4.23}$$

Here we are applying the variational formulation in (4.22) to active contours for image segmentation, so that the zero level curves of Φ can evolve to the desired features in the image. For this purpose, the energy ε_m will be defined as a functional that depends on image data, and therefore we call it as the external energy. Accordingly, the energy $\rho(\phi)$ is called the internal energy of the function Φ, since it is a function of Φ only. During the evolution of Φ according to the gradient flow (4.23) that minimizes the functional (4.22), the zero level curves will moved by the external energy ε_m but due to the penalizing effect of the internal energy, the evolving function Φ will be automatically maintained as an approximate signed distance function during the evolution according to the evolution (4.23). Thus the re-initialization procedure is completely eliminated in the proposed formulation.

In image segmentation, active contours are dynamic curves that move toward the object boundaries. To achieve this goal, we explicitly define an external energy that can move the zero level curves toward the object boundaries. Let I be an image, and g be the edge indicator function defined by

$$g = \frac{1}{1+\left|\nabla G_\sigma * I\right|^2} \tag{4.24}$$

Where G_σ is the Gaussian kernel with standard deviation σ we define an external energy for a function $\phi(x,y)$ as below [32].

$$\varepsilon_{g,\lambda,\nu}(\phi) = \lambda L_g(\phi) + \nu A_g(\phi) \tag{4.25}$$

Where $\lambda > 0$ and ν are constants, and the terms $L_g(\phi)$ and $A_g(\phi)$ are defined by

$$L_g(\phi) = \int_\Omega g\delta(\phi)\left|\nabla\phi\right| dxdy \tag{4.26}$$

and

$$A_g(\phi) = \int_\Omega gH(-\phi)dxdy \tag{4.27}$$

Where δ is the univariate Dirac function, and H is the Heaviside function. Now, we define the following total energy functional

$$\varepsilon(\phi) = \mu\rho(\phi) + \varepsilon_{g,\lambda,\nu}(\phi) \tag{4.28}$$

The external energy $\varepsilon_{g,\lambda,\nu}$ drives the zero level set toward the object boundaries, while the internal energy $\mu\rho(\phi)$ penalizes the deviation of Φ from a signed distance function during its evolution. $L_g(\phi)$ in (4.26) computes the length of the zero level curve of Φ and the energy functional $A_g(\phi)$ in (4.27) is introduced to speed up the curve evolution. The coefficient ν of A_g can be positive or negative, depending on the relative position of the initial contour to the object of interest. For example, if the initial contours are placed outside the object, the coefficient ν in the weighted area term should take positive value, so that the contours can shrink faster. If the initial contours are placed inside the object, the coefficient ν should take negative value to speed up the expansion of the contours. By calculus of variations, the Gateaux derivative (first variation) of the functional ε in (4.27) can be written as

$$\frac{\partial \varepsilon}{\partial \phi} = -\mu\left[\Delta\phi - div\left(\frac{\nabla\phi}{|\nabla\phi|}\right)\right] - \lambda\delta(\phi)div\left(g\frac{\nabla\phi}{|\nabla\phi|}\right) - \nu g\delta(\phi) \tag{4.29}$$

where Δ is the Laplacian operator. Therefore, the function Φ that minimizes this functional satisfies the Euler-Lagrange equation $\frac{\partial \varepsilon}{\partial \phi} = 0$. The steepest descent process for minimization of the functional ε is the following gradient flow:

$$\frac{\partial \phi}{\partial t} = \mu\left[\Delta\phi - div\left(\frac{\nabla\phi}{|\nabla\phi|}\right)\right] + \lambda\delta(\phi)div\left(g\frac{\nabla\phi}{|\nabla\phi|}\right) + \nu g\delta(\phi) \tag{4.30}$$

The second and the third term in the right hand side of (4.30) correspond to the gradient flows of the energy functional $L_g(\phi)$ and $A_g(\phi)$, respectively, and are responsible of driving the zero level curve towards the object boundaries.

4.3.2 Implementation

4.3.2.1 Numerical Scheme

The Dirac function $\delta(x)$ in (4.30) is slightly smoothed as the following function $\delta_\varepsilon(x)$ defined by:

$$\delta_\varepsilon(x)=\begin{cases}0, & |x|>\varepsilon \\ \frac{1}{2\varepsilon}\left[1+\cos\left(\frac{\pi x}{\varepsilon}\right)\right], & |x|\le\varepsilon\end{cases} \tag{4.31}$$

We use the regularized Dirac $\delta_\varepsilon(x)$ with $\varepsilon=$ 1.5. Because of the diffusion term introduced by our penalizing energy, no longer need the upwind scheme as in the traditional level set methods. Instead, all the spatial partial derivatives $\frac{\partial\phi}{\partial x}$ and $\frac{\partial\phi}{\partial y}$ are approximated by the central difference, and the temporal partial derivative $\frac{\partial\phi}{\partial t}$ is approximated by the forward difference. The approximation of (4.30) by the above difference scheme can be simply written as [33]

$$\frac{\phi_{i,j}^{k+1}-\phi_{i,j}^{k}}{\tau}=L\left(\phi_{i,j}^{k}\right) \tag{4.32}$$

where $L(\phi_{i,j})$ is the approximation of the right hand side in (4.30) by the above spatial difference scheme. The difference equation (4.32) can be expressed as following iteration:

$$\phi_{i,j}^{k+1}=\phi_{i,j}^{k}+\tau L\left(\phi_{i,j}^{k}\right) \tag{4.33}$$

4.3.2.2 Selection of Time Step

In implementing the proposed level set method, the time step τ can be chosen significantly larger than the time step used in the traditional level set methods. In the curve evolution large range of time step takes less number of iterations, while the curve converges to the object boundary precisely. The range of the time step τ in (4.33)

is stable if time step τ and the coefficient μ must satisfy $\tau\mu < \frac{1}{4}$ for the difference scheme described in previous Section. Using larger time step can speed up the evolution, but may cause error in the boundary location if the time step is chosen too large. There is a tradeoff between choosing larger time step and accuracy in boundary location. Usually, we use $\tau \leq 10.0$ for the most images.

4.3.3 Flexible Initialization of Level Set Function

In traditional level set methods, it is necessary to initialize the level set function Φ as a signed distance function Φ_0. If the initial level set function is significantly different from a signed distance function, then the re-initialization schemes are not able to re-initialize the function to a signed distance function. In our formulation, not only the reinitialization procedure is completely eliminated, but also the level set function Φ is no longer required to be initialized as a signed distance function. Here, we propose the following functions as the initial function Φ_0. Let Ω_0 be a subset in the image domain Ω, and $\partial\Omega_0$ be all the points on the boundaries of Ω_0, which can be efficiently identified by some simple morphological operations. Then, the initial function Φ_0 is defined as

$$\phi_0(x,y) = \begin{cases} -\rho & (x,y) \in \Omega_0 - \partial\Omega_0 \\ 0 & (x,y) \in \partial\Omega_0 \\ \rho & \Omega - \Omega_0 \end{cases}$$

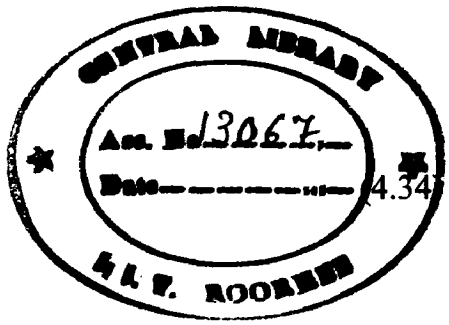

where $\rho > 0$ is a constant. Unlike signed distance functions, which are computed from a contour, the proposed initial level set functions are computed from an arbitrary region Ω_0 in the image domain Ω. Such region-based initialization of level set function is not only computationally efficient, but also allows for flexible applications in some situations.

4.4 Error Metric

The first decision for image segmentation evaluation is to choose a parameter to be compared. Parameters derived from the boundaries, such as the area enclosed or the parameter, may be compared or the boundaries themselves may be compared directly. In fetal head detection the absolute difference between the computer-generated parameter value and the user-measured parameter value which is called as distance metric is used to measure the accuracy of segmentation. This parameter compares the manually measured parameter with computer-generated parameters [34].

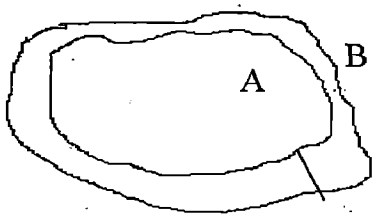

Fig 4.6 Hausdorff distance measurement

The distance metric between two curves A and B is defined as follows. When common biological landmarks are available on the two curves establishing correspondence between the curves is straightforward. In the absence of landmarks, first establish artificial correspondence between points on the two curves and then measure the distance between the corresponding points [35].

Let $A = \{a_1, a_2, ..., a_m\}$ and $B = \{b_1, b_2, ..., b_m\}$ are the set of points of two curves A and B, where a_i and b_j is an ordered pair of the x and y coordinates of a point on the curve, then the distance to the closest point(DCP)for a_i to the curve B is

$$d(a_i, B) = \min_j \|b_j - a_i\| \tag{4.35}$$

The Hausdorff distance between the two curves is defined as the maximum of the DCP's between the two curves

$$e(A,B) = \max\left(\max_i \{d(a_i, B)\}, \max_j \{d(b_j, A)\} \right) \tag{4.36}$$

The closest point distance associates each point on both curves to a point on the curve, and the Hausdorff distance finds the largest distance between the associated points.

CHAPTER 5

RESULTS AND DISCUSSIONS

This work is carried out on AMD 64 processor PC operating at1.8 GHz clock. The program for detection of fetal head using different techniques has been implemented in Matlab 7.0.1. The image database has been taken from GE health care. The results of active contours without re-initialization which is combined with the randomized Hough transform are compared with the basic level set method implemented through Mumford-Shah function also called as active contours with out edges. The corresponding accumulator values of randomized Hough transform for ellipse creation are tabulated. The segmented output is compared with actual fetal head location and an error metric called Hausdorff distance is calculated for every image.

5.1 Results of Basic Method with Mumford-Shah function:

In this method, first of all, a circle is initialized inside the fetal head and depending upon the signed distance function and some energy equations, this initial contour is moved towards the boundary and the final segmented output is compared with the hand-outlined fetal head. The results are shown in Figs 5.1(a)-(f). This method is also called as active contours without edges because it does not require the edge indicator function.

(a)

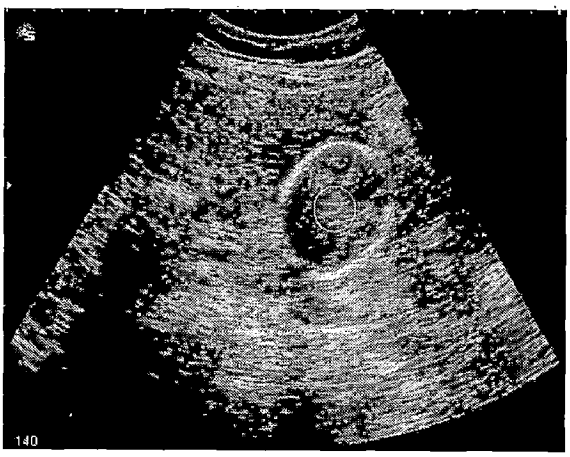

(b)

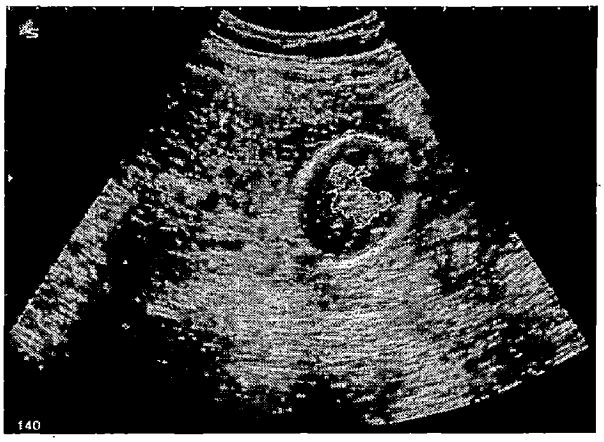

(c)

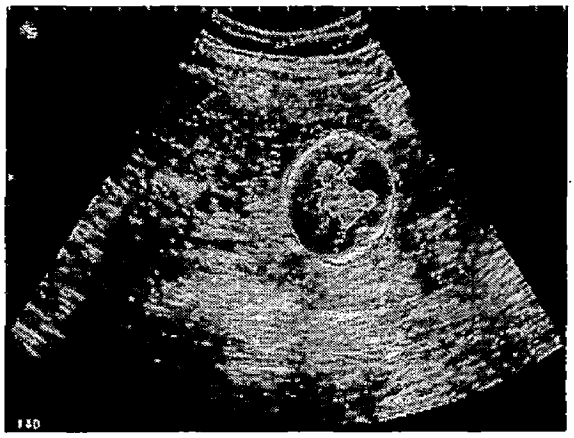

(d)

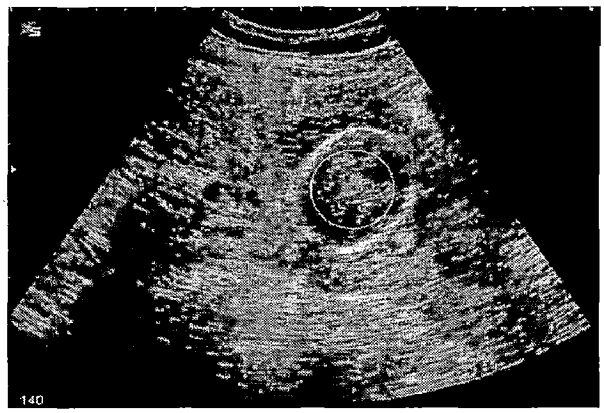

(e)

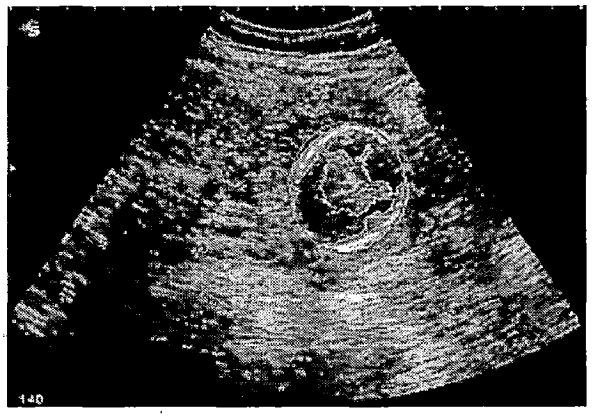

(f)

Fig 5.1 (a) Original image of fetal head 1 (b) Initial level set function as the signed distance to a circle 1 (c) Segmented output of fetal head 1 after 100 iterations (d) Segmented output compared with the hand-outlined fetal head (e) Initial level set function as the signed distance to a circle 2 (f) Segmented output compared with the hand-outlined fetal head 1 after 100 iterations

As it is observed from the figure, required fetal head is not detected and unnecessary splitting has occurred. Hausdorff distance for this result is 38.031.

From this result, it is evident that in this method the final segmented output is totally dependent on the initial position of the circle. For the same fetal head image, it gives different results due to the different initialized positions of the circle. Fig 5.1 (d)

indicates the false detection of the fetal head while Fig 5.1 (f) shows that the final output is split into different regions even though it is not required so some unnecessary splitting has taken place in this method. The Hausdorff distance indicates the distance between the segmented output of our method to the hand-outlined fetal head which is relatively a large value.

Fig 5.2 (a)-(f) presents another result. Here, required fetal head is detected but more number of iterations may result in cross over of boundaries. The Hausdorff distance is obtained as 16.098 which shows a better approximation fetal head periphery.

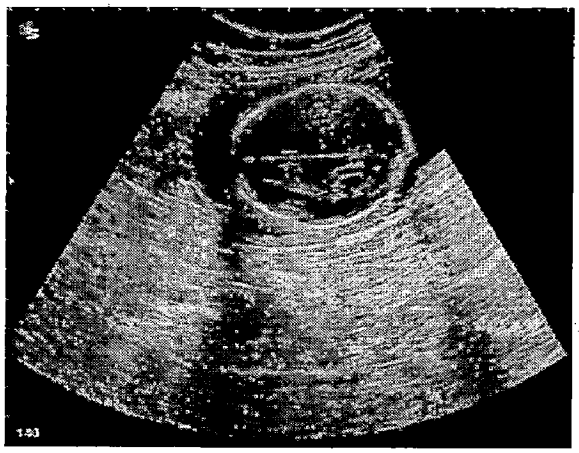

(a)

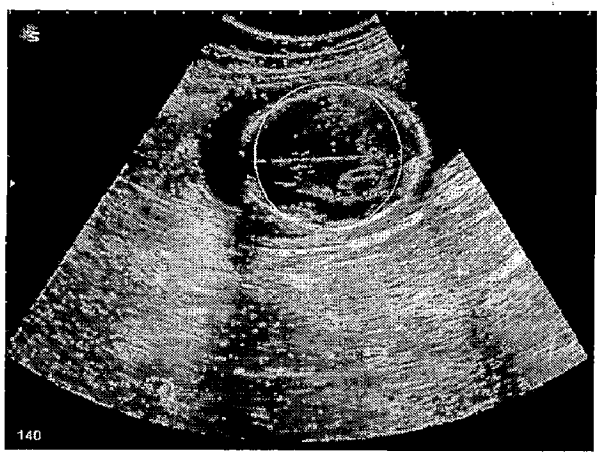

(b)

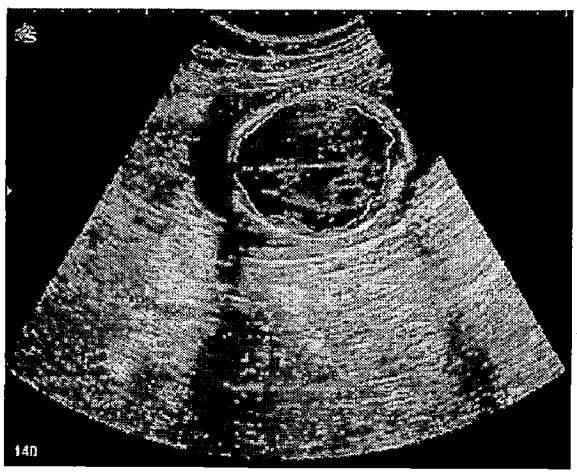

(c)

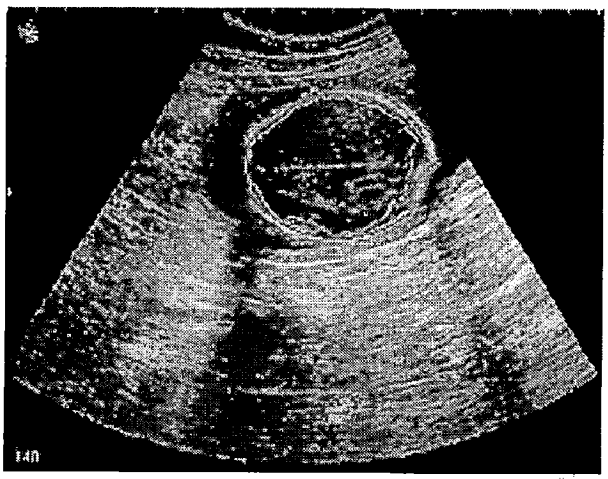

(d)

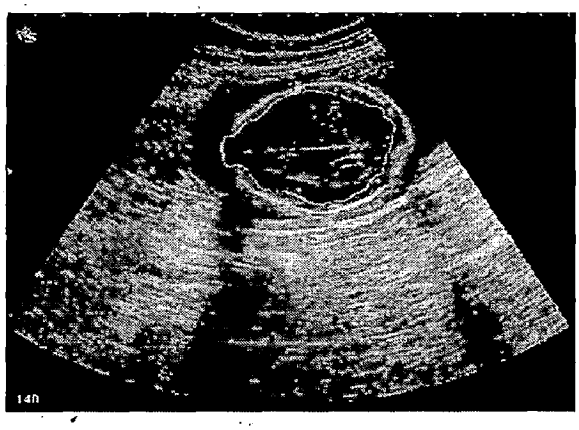

(e)

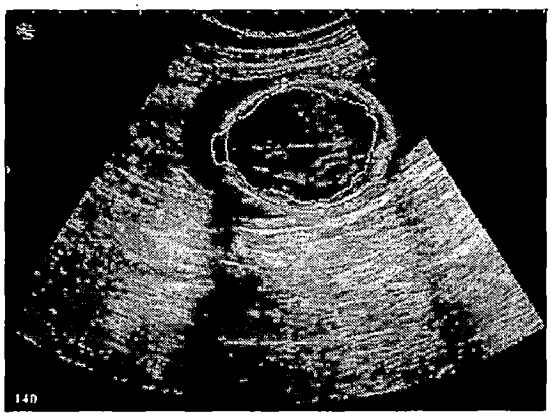

(f)

Figure 5.2 (a) Original image of fetal head 2 (b) Initial level set function as the signed distance to a circle. (c) Segmented output of fetal head 2 after100 iterations (d) Segmented output compared with the hand-outlined fetal head after 100 iterations (e) Segmented output of fetal head 2 after 150 iterations. (f) Segmented output compared with the hand-outlined fetal head 2 after 150 iterations

Here again, from the results, it is evident that in this method the final segmented output is totally dependent on the initial position of the circle. Fig 5.2(d) shows the properly segmented fetal head i.e. if the circle is initialized in proper position this method can detect the required fetal head accurately. Further Fig 5.2 (e) shows that if number of iterations are increased the output crosses the required boundaries. Similar results have also been obtained for more images.

Fig 5.3 (a)-(c) presents another result. Hausdorff distance for this result is 27.238.

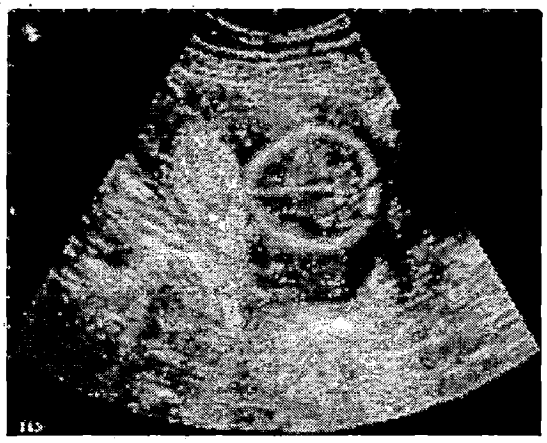

(a)

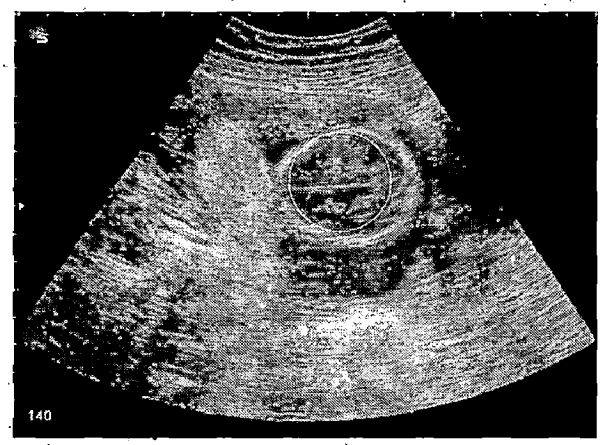

(b)

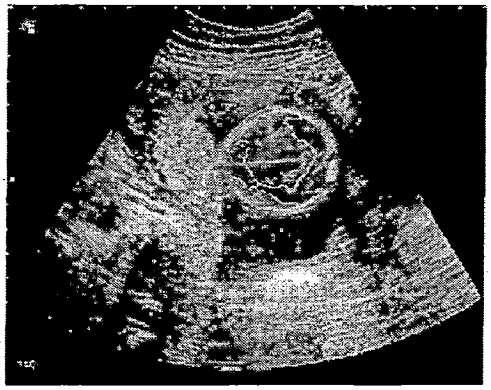

(c)

Figure 5.3 (a) Original image of fetal head 3 (b) Initial level set function as the signed distance to a circle. (c) Segmented output of fetal head3 after100 iterations

In general, it can be said that the segmentation of the ultrasound images by the basic method with Mumford-Shah function, which is also called as the active contours without edges, will give results depending on the position of the initial circle and sometimes unnecessary splitting also takes place during the evaluation of the curve. If the circle is located in proper position, then it produces properly segmented output.

5.2 Results of Active contours without re-initialization with randomized Hough transform:

Figs. 5.4 (a)-(j) presents the results for one of the fetal head image. Here, the required fetal head is properly detected. It has Hausdorff distance of 6.198. Table 5.1 presents the accumulator values of randomized Hough transform.

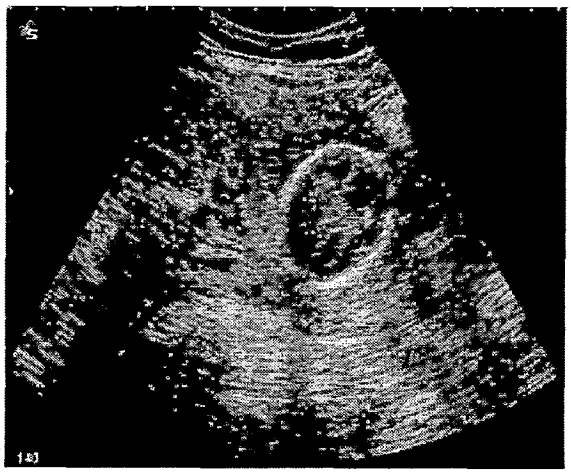

(a)

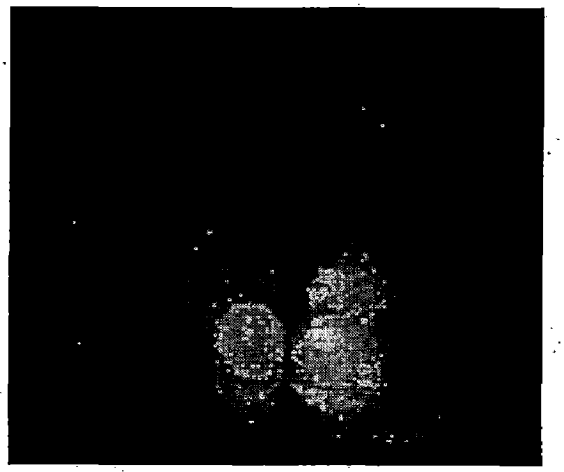

(b)

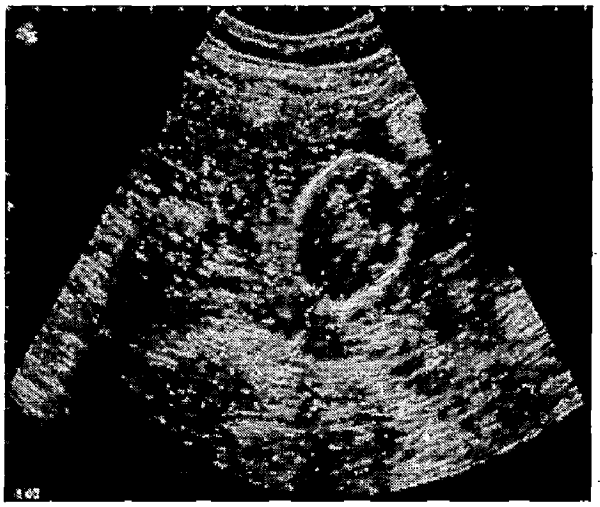

(b)

(d)

(e)

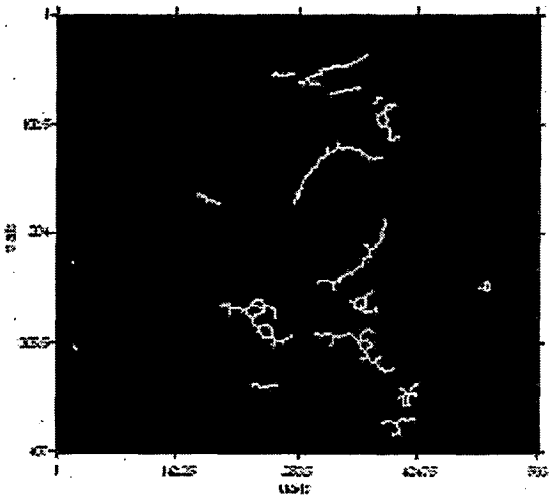

(f)

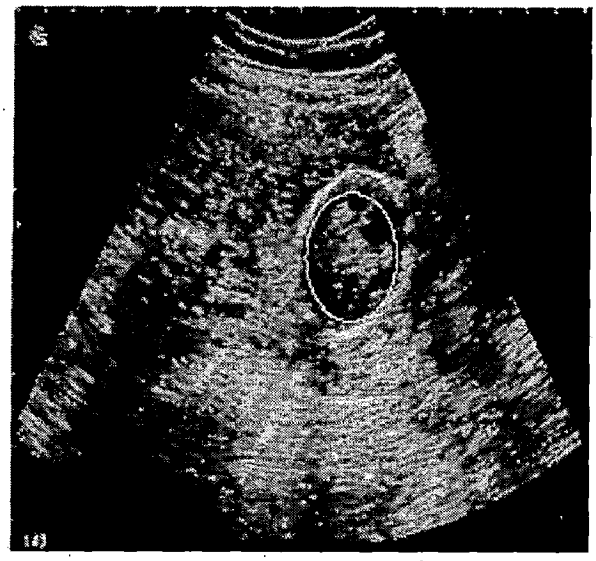

(g)

(h)

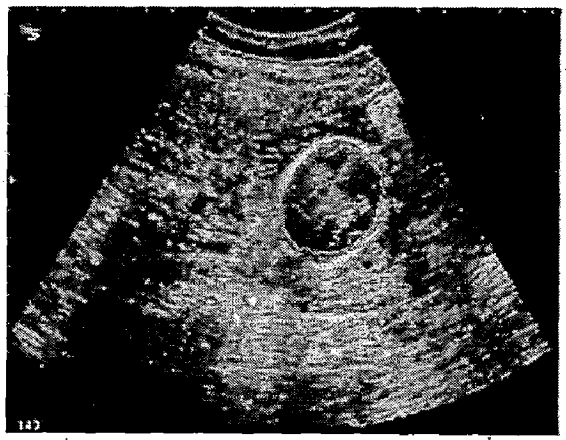

(i)

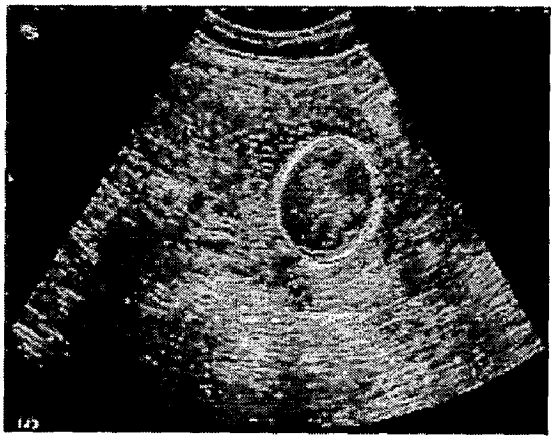

(j)

Figure 5.4 (a) original image of fetal head 1 (b) image after opening (c) image after closing (e) Skeleton image (f) image after spurring (g) ellipse creation by RHT (Randomized Hough Transform) (h) segmented output after 25 iterations (i) segmented output after 50 iterations (j) segmented output compared with Hand-outlined fetal head

Table 5.1 Accumulator values of randomized Hough transform for fetal head 1

X_0	Y_0	a	b	score
205.4291	319.6688	45.9978	59.8510	20
158.0100	341.2037	34.4716	64.4716	18
324.6535	206.4843	37.9293	52.8779	09
192.8236	330.9789	39.9413	65.5170	25
206.3451	319.1888	42.2665	60.4442	20
162.2502	340.9509	47.0750	67.9154	45
169.3690	337.8159	44.9155	59.8758	36
196.6888	329.0470	49.4738	60.9248	34
164.0216	339.4861	48.3230	66.1465	38
178.7859	332.6517	47.6855	43.3434	67

From this result it can be said that by initializing the ellipse by RHT, which is necessary initial step for the further curve evaluation in level set method, it can detect the fetal head with in few iterations. Here after reaching the boundaries even though the number of iterations are increased it does not cross the boundaries i.e. stopping criteria is also good in this case.

Fig 5.5(a)-(j) presents another result of this method. In this case too, fetal head is detected with less number of iterations. Hausdorff distance in this case is 5.736 which indicates a good quality segmentation. Table 5.2 presents the accumulator values for this image.

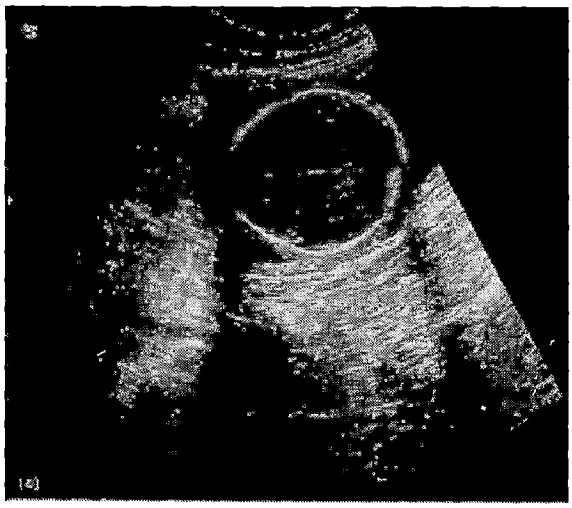

(a)

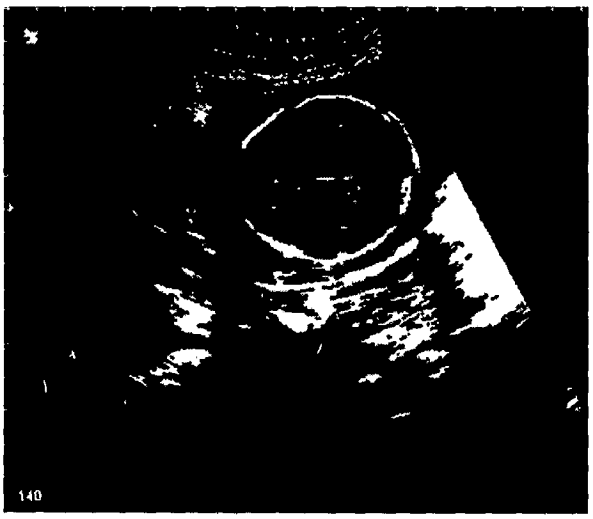

(b)

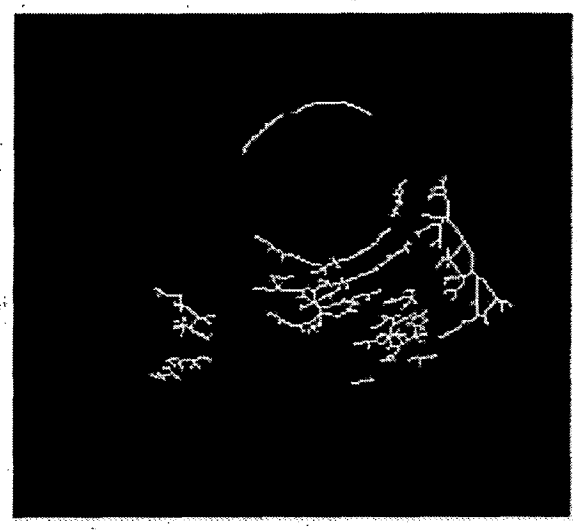

(c)

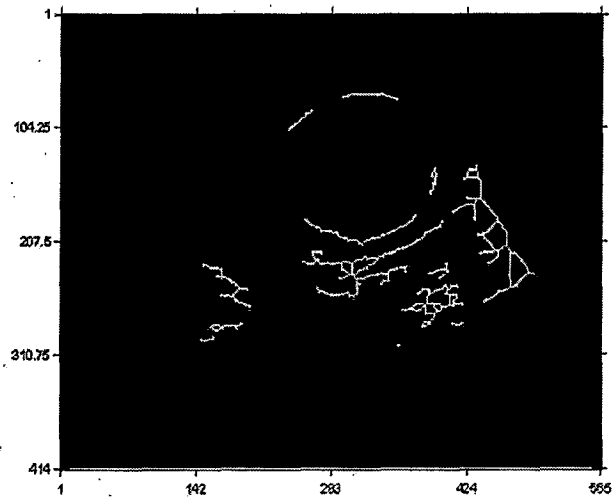

(d)

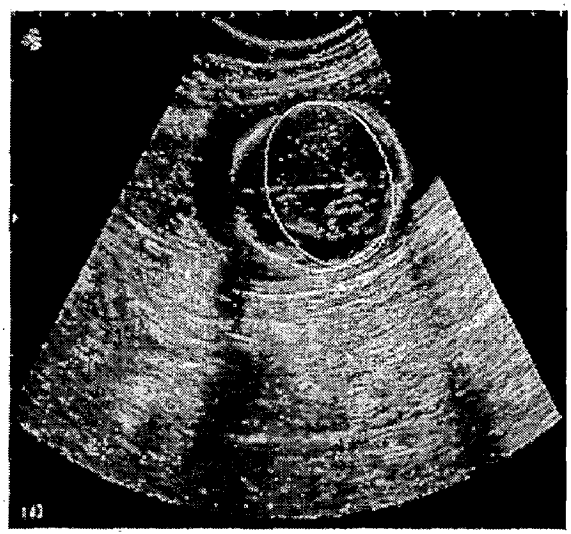

(e)

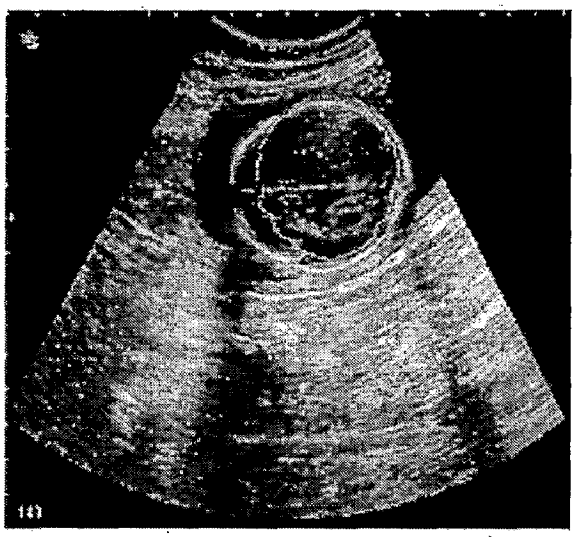

(f)

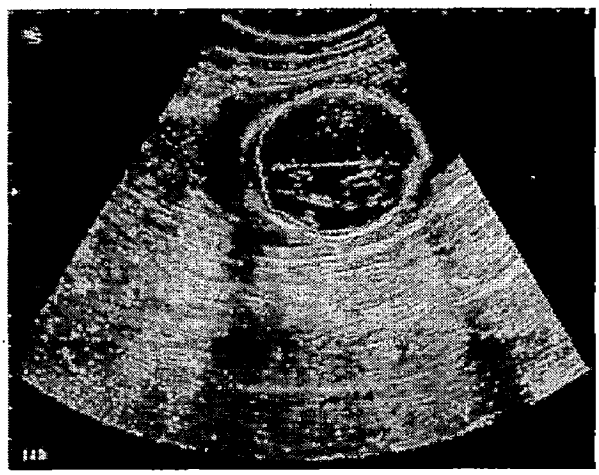

(g)

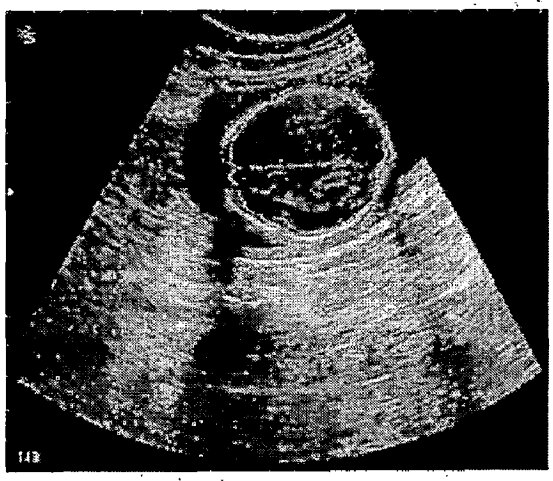

(h)

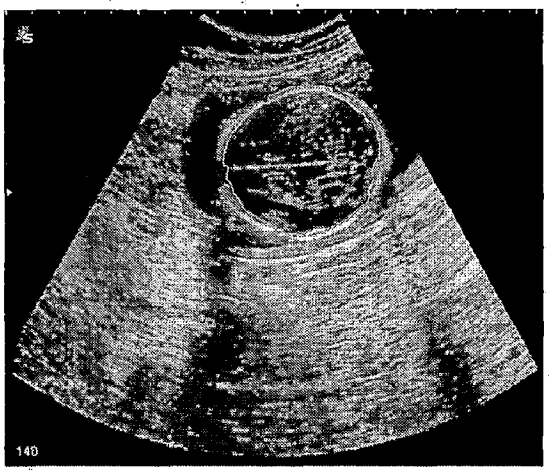

(h)

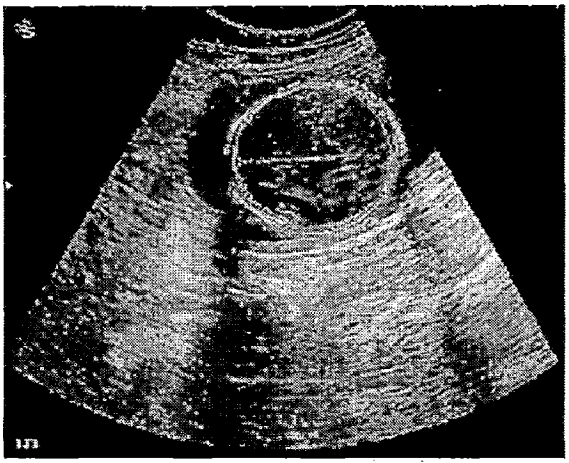

(j)

Fig 5.5 (a) original image of fetal head 2 (b) binary image (c) skeleton image (d) image after spurring (e) ellipse creation by RHT (f)segmented output after 25 iterations (g) segmented output after 50 iterations (h) segmented output after 75 iterations (i) segmented output after 75 iterations (j) segmented output with hand outlined fetal head

Table 5.2 Accumulator values of randomized Hough transform for fetal head 2

X_0	Y_0	a	b	score
308.5465	190.4043	50.3886	76.5035	10
283.5930	236.1139	41.1987	79.6138	12
238.5950	276.5506	54.3499	73.7554	10
303.4106	173.7731	61.5578	83.4845	15
321.8329	144.8148	45.3426	89.8873	12
327.5702	138.0464	49.2695	83.5460	11
320.8661	142.2578	57.6197	85.5466	18
187.3859	306.9329	63.3617	79.4742	11
303.4840	175.1854	66.2208	83.3659	16
134.7308	326.1830	70.1863	51.0914	19

From this results too, it can be said by initializing the ellipse by RHT and by choosing non-zero pixels from the skeleton of the original image which is necessary initial step for the further curve evaluation in level set method. The fetal head is detected within few iterations. The distance metric too has less value indicating that fetal is accurately detected.

Similar results are also obtained for many more images. Fig 5.6 (a)-(e) presents another result. Hausdorff distance for this result is 3.673.

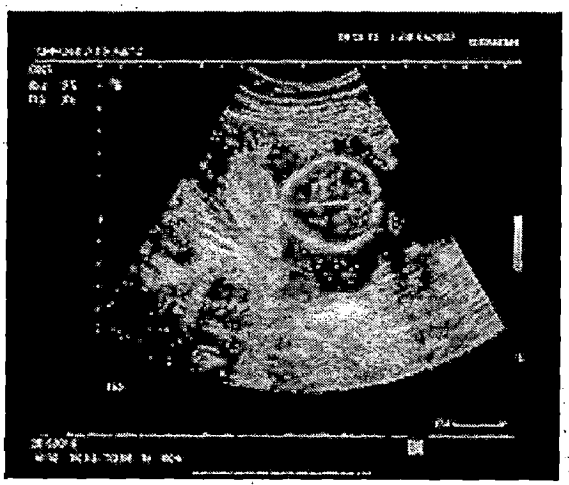

(a)

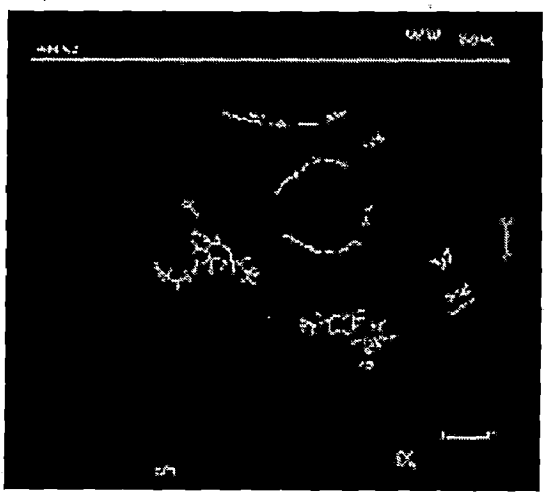

(b)

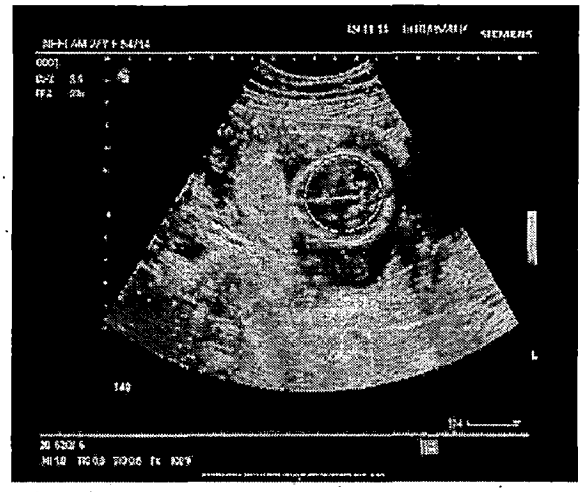

(b)

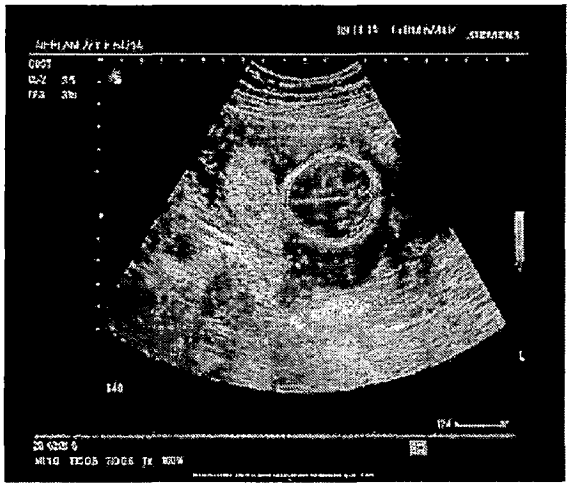

(d)

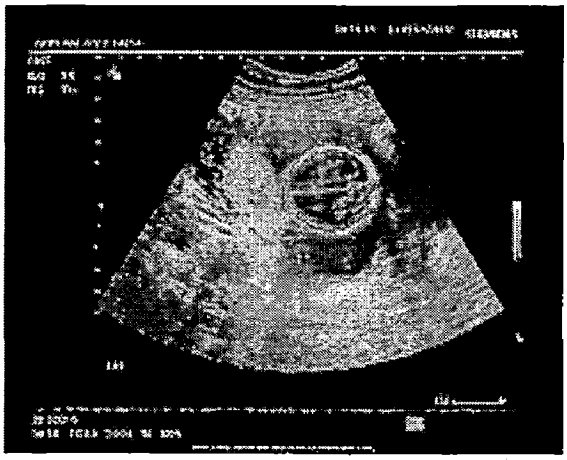

(e)

Figure 5.6 (a) original image of fetal head 3 (b) skeleton image (c) ellipse creation by RHT (d) segmented output after 50 iterations (e) segmented output with hand outlined fetal head

Table 5.3 Accumulator values of randomized Hough transform for fetal head 3

X_0	Y_0	a	b	score
219.2147	285.8300	60.5152	77.9422	08
123.9824	343.0512	59.8063	65.4122	22
121.3931	345.1179	59.7081	62.6928	18
255.5228	212.0410	12.9318	38.8116	05
125.1663	337.7852	62.1434	77.4499	15
167.3097	321.7960	61.0057	70.4126	24
164.0649	287.9348	21.6917	39.6454	13
164.6647	326.4348	57.4017	80.8704	10
117.1485	341.0095	60.5718	87.7250	19
167.2238	323.4008	58.8466	81.9889	16

The level set method with randomized Hough transform has been implemented on many more images, results are shown from Fig 5.7 -5.9. A summarized result for the same is presented in Table 5.4.

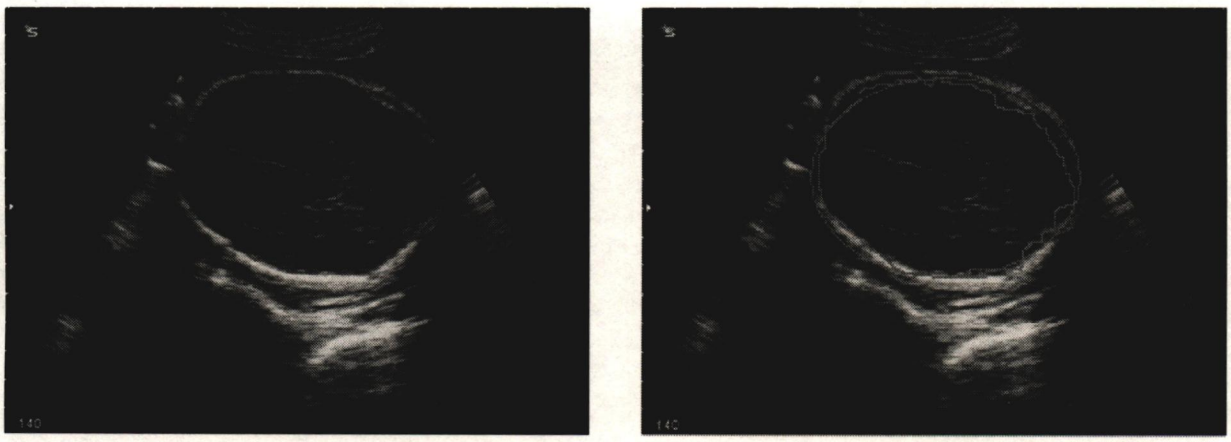

(a) (b)

Fig 5.7. (a) original image of fetal head 4 (b) Segmented output with hand outlined fetal head after 50 iterations.

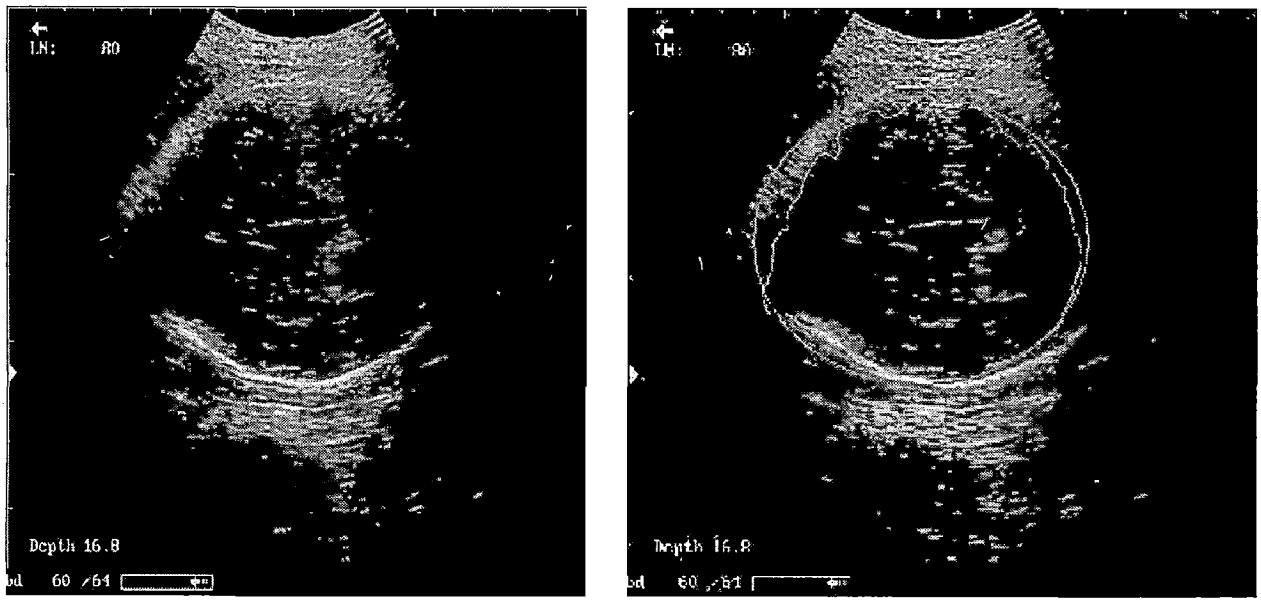

(a) (b)

Fig 5.8. (a) original image of fetal head 5 (b) Segmented output with with hand outlined fetal head after 50 iterations.

(a) (b)

Fig 5.9. (a) original image of fetal head 6 (b) Segmented output with with hand outlined fetal head after 50 iterations

Table 5.4 Comparison of Hausdorff distance for the images from Fig 5.4 – 5.9

Image No	No. of iterations used for head detection	Hausdorff distance
1	50	6.198
2	75	5.736
3	50	3.673
4	50	8.604
5	50	14.435
6	50	10.23

CHAPTER 6
CONCLUSIONS AND SCOPE FOR FUTURE WORK

6.1 Conclusions

Two different approaches of level set method have been implemented here. One is active contour without reinitialization combined with randomized Hough transform and the other is basic level set method implemented through Mumford-Shah function, which is also called as active contours without edges. It is concluded that the active contour model without edges based on the Mumford-Shah function is fully dependent on the initial position of the curve. It crosses the required boundaries if the number of iterations are more and also results in unnecessarily splitting of the curve during the propagation of the curve. The detection of fetal head by using level set method of active contours without edges experiences some problems like the output dependency on initial position of curve which has to be given by the user. This means that initial contour position given by different users will lead to different segmented output. This method will produce accurate result if initial curve is initialized in proper position i.e. user should have the knowledge about the region where he has to initialize the circle.

The randomized Hough transform creates the ellipse by just specifying the region of interest in proper position in the images i.e. it gives the proper initial curve from where level set method active contours without reinitialization starts to get the proper segmentation. The initial curve is the basic step for level set method and RHT is creating the ellipse accurately in the required position i.e. inside the required fetal head.

The randomized Hough transform accurately discriminates the ellipses and non-ellipse objects. It has the ability to find the ellipses even in the noisy images. It also needs less memory space and is computationally efficient. The required memory size is also less because here in accumulator only those ellipse parameters are stored which are repeated maximum number of times i.e. here unnecessary memory storage is avoided.

The ellipse which is created by the randomized Hough transform is given as initial input to the level set method of active contours without re-initialization which segments the fetal head in our ultrasound images effectively by overcoming the limitations of previous method. After creation of the ellipse it is evolving towards the required boundaries and it does not require any reinitializations in further steps. In this method even for more iterations generated contour does not cross the fetal head boundaries indicating that the stopping criteria is also good in this method.

6.2 Scope for Future work

As far as the future directions of this dissertation work are concerned, the validation of the framework using other fetal head detection applications can be considered. Furthermore, the proposed segmentation model can be extended to make this method as automatic.

An important extension to the image segmentation approach can be its application to colour images and real-world images. The automatic selection of the region of interest based on the input image and the some image dependent criteria completely will make this method fully automatic.

REFERENCES

1. Eng. Christine W. Hanna, Prof. Abou Bakr M. Youssef," *Automated Measurements in Obstetric Ultrasound Images"* Scientific Ultrasound Center, Cairo, Egypt, 1997 IEEE

2. Gonzalez, R.C., Woods, R.E.,"*Digital Image Processing*", Addison Wesley publishing Company, Inc., 1993.

3. Suhuai Luo and Jessi S.jin,"*Recent Progresses on Cerebral Vasculature Segmentation for 3D Quantification and Visualization of MRA*", Proceedings of the Third International Conference on Information Technology and Applications, 2005 IEEE

4. P.Lin, F.Zhang, Y.yang, and C.Zheng."*Carpal-bone feature extraction analysis in skeletol age assessment based on deformable model*", Journal of Computer Science and Technology, 2004.

5. Chenyang Xu, Anthony Yezzi, Jerry L. Prince," *On the Relationship between Parametric and Geometric Active Contours",* In Proc. of 34th Asilomar Conference on Signals, Systems, and Computers, pp. 483-489, October 2000

6. R.Durikovic, K. Kaneda, and H. Yamashita. "*Dynamic contour:a texture approach and contour operations*". The Visual Computer, 11:277–289, 1995.

7. C. Xu and J. L. Prince. "*Snakes, shapes, and gradient vector flow*".IEEE T. Imag. Proc., 7(3):359–369, 1998.

8. J. E. Balland L.M. Bruce," *Level Set Segmentation of Remotely Sensed Hyperspectral Images",* 2005 IEEE.

9. M. Sussman, P. Smereka, and ***S.*** Osher. "*A level set approach fir computing solutions to incompressible two-phase flow,"* J. of computational Physics, 114146-159, 1994.

10. Mohamed Sabry, Charles B. Sites, Aly A. Farag, Stephen Hushek, and Thomas Moriarty *"Statistical Cerebrovascular Segmentation for Phase-Contrast MRA Data,"* Proc. of the 1st International Conf. on Biomedical Engineering, Cairo, Egypt,December, 2002.

11. J.A.Sethian,"*Level Set Methods and Fast Marching Methods*", Cambridge University Press, 2005.

12. Zhiguo Cheng, Yuncai Liu," *Efficient Technique for Ellipse Detection Using Restricted Randomized Hough Transform",* Proceedings of the International

Conference on Information Technology: Coding and Computing (ITCC'04), 2004 IEEE

13. Lei XU, Erkki OJA, and Pekka Kultanena. "*A new curve detection method: Randomized hough transforms (rht)*". Pattern Recognition Letters, (11):331–338, 1990.

14. David Manura. Dave's math tables: Conic sections.

15. Weilu, Jinglu Tan and Randall Floyd, "*Automated Fetal Head Detection and Measurement in Ultrasound Images by Iterative Randomized Hough Transform*", Ultrasound in Med. & Biol., Vol. 31, No. 7, pp. 929–936, Elsevier,2005

16. A.Goneid,"*A Method for the Hough Transform Detection of circles and Ellipses using a 1-Dimensional Array*", 1997 IEEE

17. Robert A.McLaughlin,"*Randomized Hough Transform: Improved ellipse detection with comparison*", Pattern Recognition Letters 19(1998)299-305, 1998 Elsevier

18. Heikki Kalviainen,"*An extension to the Randomized Hough Transform exploiting connectivity*", Pattern Recognition Letters 18(1997) 77-85, 1997 Elsevier

19. A.S.Aguado, M.E.Montiel and M.S.Nixon,"*Ellipse Detection via Gradient Direction in the Hough Transform*", 1995 IEEE

20. Nick Bennett, Robert Burridge, and Naoki Saito,"A method to detect and characterize ellipses using the Hough Transform", 1999 IEEE

21. G.K.Matsopoulos and S.Marshal,"*Medical Applications of Mathematical Morphology*", 1993 IEEE

22. Leavers VF. , "The dynamic generalized Hough transform: Its relationship to the probabilistic Hough transforms and an application to the concurrent detection of circles and ellipses", CVGIP Image Understanding 1992; 56(3):381–398.

23. Lu W.," Hough transforms for shape identification and applications in medical image processing". PhD dissertation. Columbia, MO: University of Missouri - Columbia, 2003.

24. Xu L, Oja E., "*Randomized Hough transform (RHT): Basic mechanisms, algorithms, and computational complexities*", CVGIP Image Understanding 1993; 57(2):131–154.

25. Xu L, Oja E, Kultanen P.," *A new curve detection method: Randomized Hough transform (RHT)*", Pattern Recogn Lett 1990; 11:331–338.

26. Tony F. Chan, and Luminita A. Vese," Active Contours Without Edges", IEEE Transactions on Image Processing, VOL. 10, NO. 2, February 2001 IEEE

27. S. Osher and J. A. Sethian, "*Fronts propagating with curvature-dependent speed: Algorithms based on Hamilton–Jacobi Formulation*," J.Comput. Phys., vol. 79, pp. 12–49, 1988

28. H.-K. Zhao, T. Chan, B. Merriman, and S. Osher, "*A variational level set approach to multiphase motion*," J. Comput. Phys., vol. 127, pp.179–195, 1996.

29. L. C. Evans and R. F. Gariepy," *Measure Theory and Fine Properties of Functions"*. Boca Raton, FL: CRC, 1992.

30. D. Mumford and J. Shah, "*Optimal approximation by piecewise smooth functions and associated variational problems*," Commun. Pure Appl.Math, vol. 42, pp. 577–685, 1989.

31. Chunming Li, Chenyang Xu, Kishori M. Konwar, Martin D. Fox." *Fast Distance Preserving Level Set Evolution for Medical Image Segmentation*", 2006 IEEE

32. C. Li, C. Xu, C. Gui, and M. D. Fox. ,"*Level set formulation without re-initialization: a new variational formulation*". Proc. 2005 IEEE CVPR, 1:430–436, San Diego, 2005.

33. J. A. Sethian. *Level Set Methods and Fast Marching Methods*. Cambridge University Press, Cambridge, 1999.

34. Vikram Chalana and Yongmin Kim," *A Methodology for Evaluation of Boundary Detection Algorithms on Medical Images* ", IEEE Transactions on Medical Imaging, VOL. 16, NO. 5, October 1997

35. D. P. Huttenlocher, G. A. Klanderman, and W. J. Rucklidge, "*Comparing images using the Hausdorff distance*," IEEE Trans. Pattern Anal.Machine Intell., vol. 15, pp. 850–863, 1993.